

Supporting Information for:
Convolutional Neural Networks and Volcano Plots:
Screening and Prediction of Two-Dimensional Single-Atom
Catalysts for CO₂ Reduction Reactions

1 Additional details on DFT calculations

1.1 Catalyst models

Representative structures for each substrate are depicted in Figure 2 through Figure 7. For the adsorption process, the initial state is defined by positioning the optimized adsorbates at a distance of 6.5 Å from the single-metal atoms supported on the substrate, oriented along the z-axis.

The periodic table shows the following color coding for investigated elements:

- Transition metals (Sc, Ti, V, Cr, Mn, Fe, Co, Ni, Cu, Zn, Sc, Ti, V, Cr, Mn, Fe, Co, Ni, Cu, Zn, Y, Zr, Nb, Mo, Tc, Ru, Rh, Pd, Ag, Cd, In, Sn, Sb, Te, I, Xe, La, Hf, Ta, W, Re, Os, Ir, Pt, Au, Hg, Tl, Pb, Bi, Po, At, Rn, Ac, Rf, Db, Sg, Bh, Hs, Mt, Ds, Rg, Cn, Nh, Fl, Mc, Lv, Ts, Og) are highlighted in blue.
- Metalloids (B, C, N, O, F, Si, P, S, Cl, Ar, Ge, As, Se, Br, Kr) are highlighted in purple.
- Other metals (H, He, Li, Be, Na, Mg, K, Ca, Rb, Sr, Cs, Ba, Fr, Ra) are highlighted in orange.

Figure 1: Periodic table of investigated metals. Periodic table highlighting investigated elements: transition metals in blue, metalloids in purple, and other metals in orange.

1.2 CO₂RR pathways

In this study, we explored three reaction pathways that have been previously documented in the literature [2, 5, 7], as depicted in Figure 8. The adsorption configuration of the *CHO intermediate is pivotal in each of these pathways for determining the reaction mechanism in the CO₂RR process. We calculated the energies associated with the *CHO intermediate for catalysts supported on g-C₃N₄, nitrogen-doped graphene, and dual-vacancy graphene-under each mechanism. These calculations are summarized in section 1.2. Our results indicate that Pathway 1 is the most energetically favorable for most catalysts we investigated. Therefore, to streamline our analysis, we focused exclusively on Mechanism 1 across all catalysts examined.

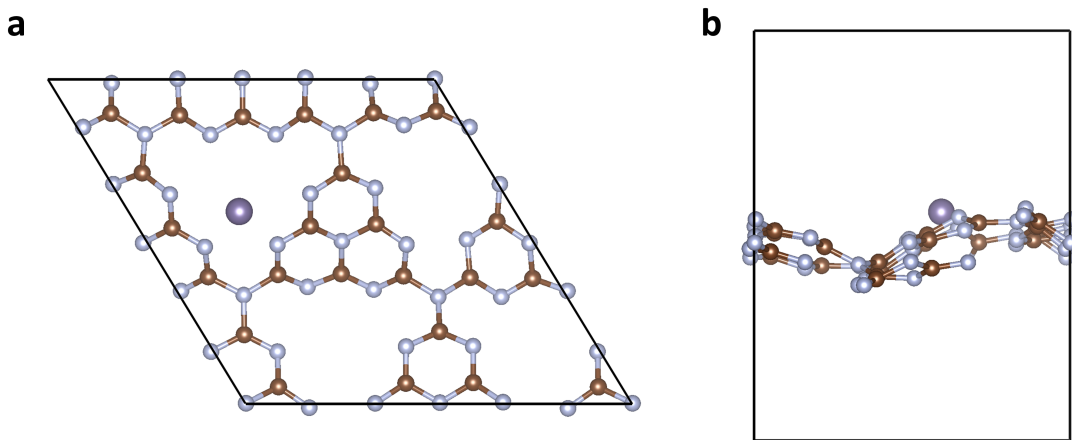


Figure 2: Structure of single germanium atom supported on graphitic nitride. (a) View along the z-axis and (b) view along the x-axis of the $\text{Ge@g-C}_3\text{N}_4$ structure. In the illustrations, silver spheres represent N atoms, brown spheres signify C atoms, and purple sphere indicates Ge atom.

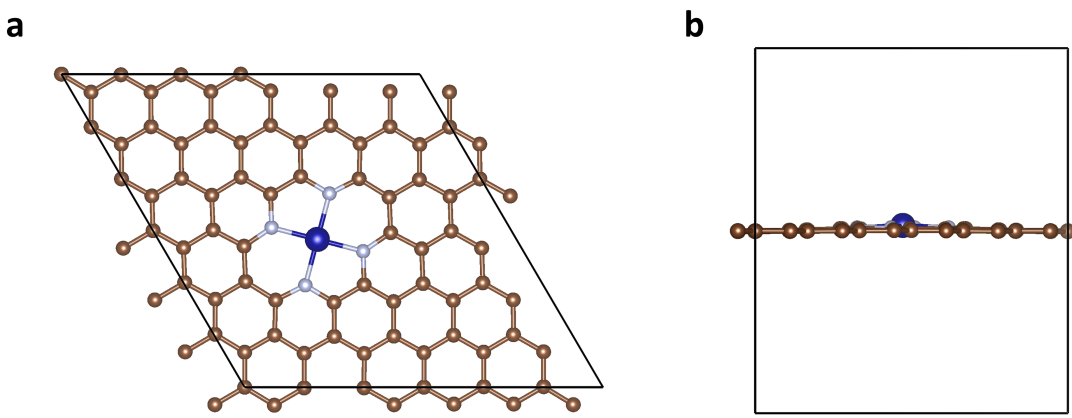


Figure 3: Structure of single chromium atom supported on nitrogen-doped graphene. (a) View along the z-axis and (b) view along the x-axis of the $\text{Cr@nitrogen-doped-graphene}$ structure. In the illustrations, silver spheres represent N atoms, brown spheres signify C atoms, and indigo sphere indicates Cr atom.

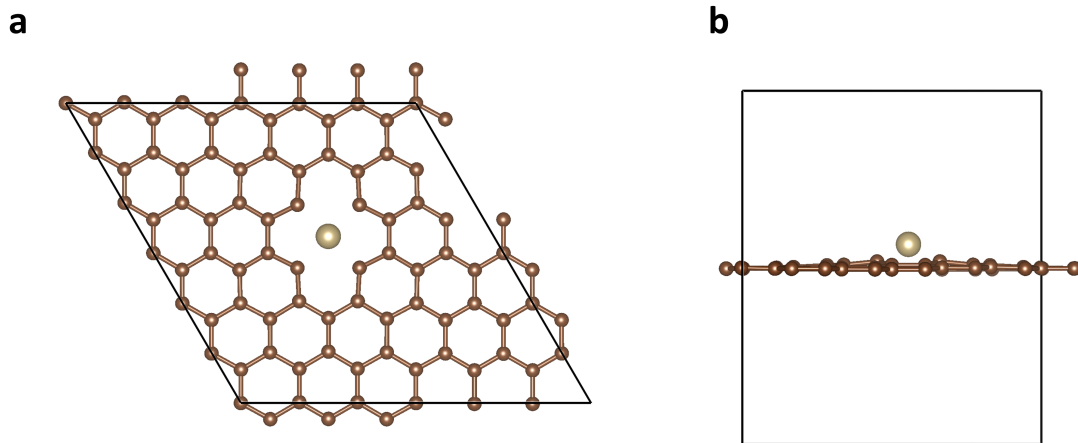


Figure 4: Structure of single osmium atom supported on graphene with dual-vacancy. (a) View along the z-axis and (b) view along the x-axis of the Os@graphene-with-dual-vacancy structure. In the illustrations, brown spheres signify C atoms, and light yellow sphere indicates Os atom.

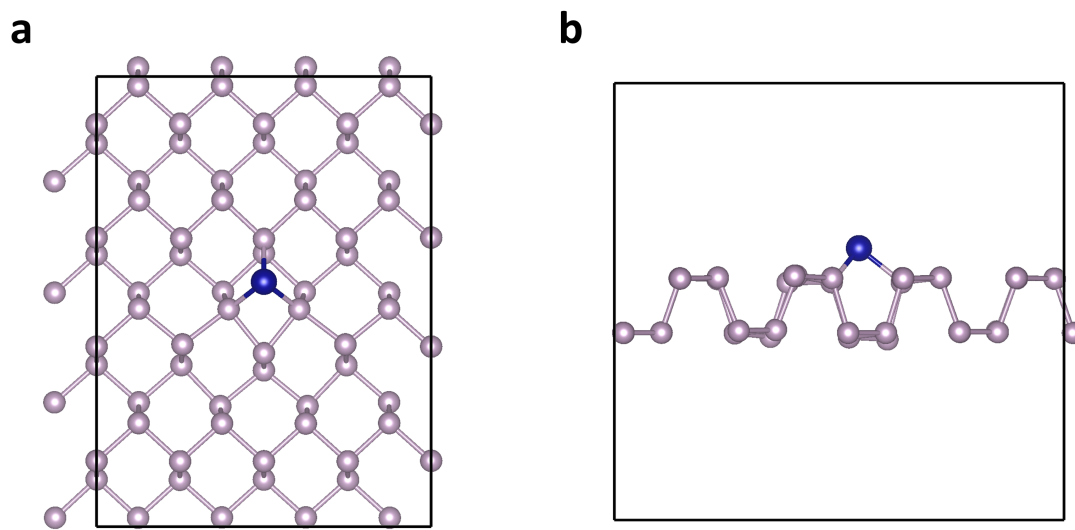


Figure 5: Structure of single chromium atom supported on black phosphorous. (a) View along the z-axis and (b) view along the x-axis of the Cr@black phosphorous structure. In the illustrations, light purple spheres represent P atoms, and indigo sphere indicates Cr atom.

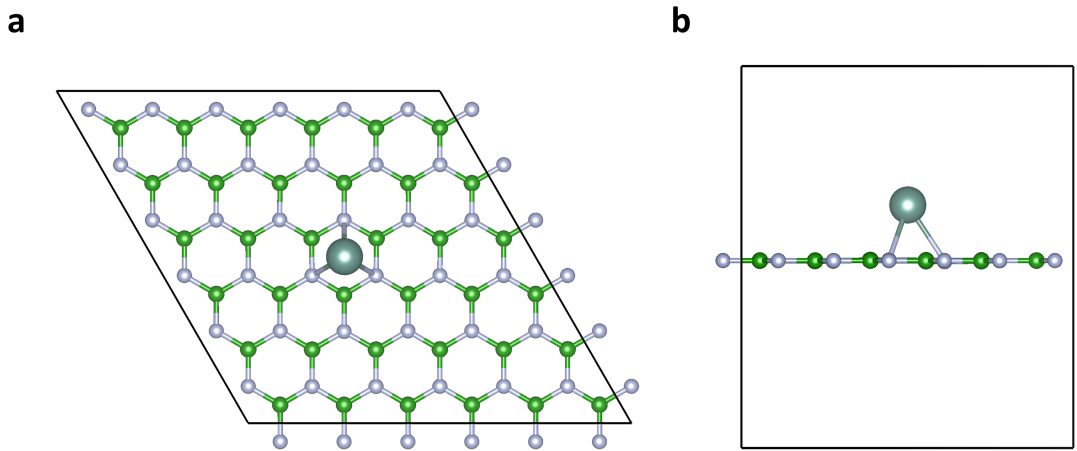


Figure 6: Structure of single yttrium atom supported on boron nitride. (a) View along the z-axis and (b) view along the x-axis of the Y@boron-nitride structure. In the illustrations, silver spheres represent N atoms, green spheres signify B atoms, and light green sphere indicates Y atom.

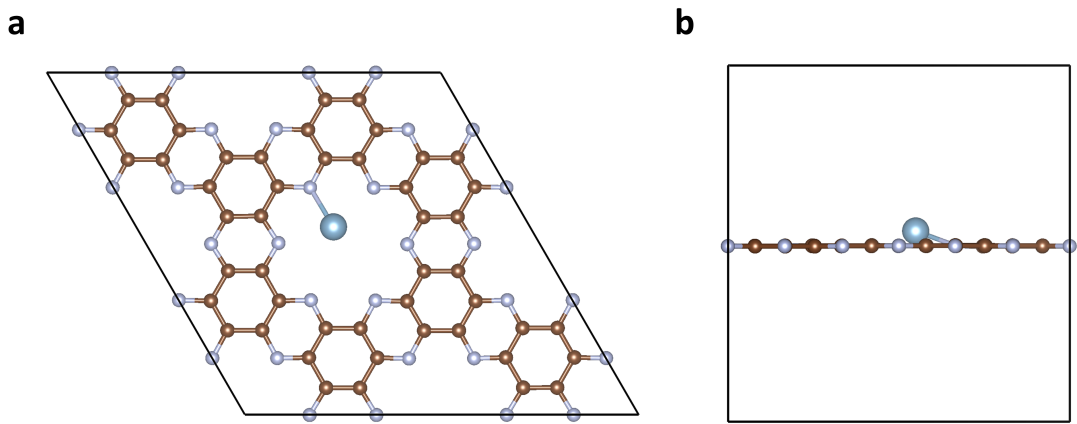


Figure 7: Structure of single aluminum atom supported on C_2N . (a) View along the z-axis and (b) view along the x-axis of the Al@ C_2N structure. In the illustrations, silver spheres represent N atoms, brown spheres signify C atoms, and blue sphere indicates Al atom.

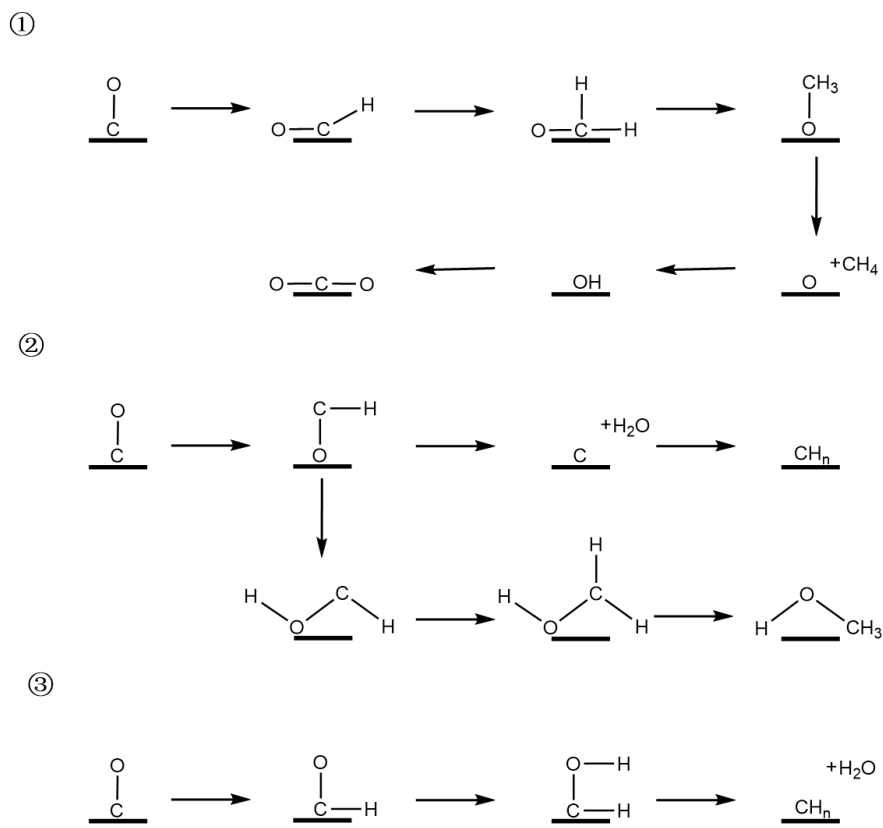


Figure 8: Three investigated CO_2RR pathways [2, 5, 7] investigated in this work.

Table 1: DFT-calculated energies in eV for protonated *CO intermediate for three investigated CO₂RR pathways.

Metal	g-C ₃ N ₄			nitrogen-doped graphene			graphene with dual-vacancy		
	Pathway-1	Pathway-2	Pathway-3	Pathway-1	Pathway-2	Pathway-3	Pathway-1	Pathway-2	Pathway-3
Al	-499.3494	-497.8343	-499.3005	-670.3489	-668.5142	-670.3093	-667.2538	-666.6725	-667.2665
Co	-502.5946	-501.1257	-502.6139	-672.8847	-670.8013	-672.9020	-671.6284	-670.4388	-671.3827
Cr	-505.6012	-504.2022	-505.6029	-675.3126	-674.1640	-675.3480	-673.4283	-672.1919	-673.3818
Cu	-495.8913	-493.6853	-495.8820	-666.9894	-664.9810	-666.9705	-666.9876	-664.7684	-667.1395
Fe	-501.3325	-499.3969	-501.3221	-673.8242	-672.0887	-673.8478	-672.7810	-671.5694	-672.4960
Ga	-498.2365	-496.3967	-498.2912	-667.3963	-665.4677	-667.3482	-665.7780	-664.8573	-665.8030
Ge	-500.2052	-497.9780	-500.2156	-668.1785	-666.3484	-668.1463	-667.7387	-665.7394	-667.7324
Mn	-502.6355	-500.8006	-502.6294	-674.6848	-672.9574	-674.7030	-673.2243	-672.6495	-673.2361
Ni	-500.4085	-498.5165	-500.3985	-670.0979	-667.9544	-670.0832	-670.1619	-668.3684	-670.1756
Sc	-503.4428	-501.6129	-503.4437	-673.9590	-671.7624	-673.3818	-670.0841	-668.1044	-669.6050
Ti	-503.7848	-502.6148	-503.8033	-675.1006	-673.2417	-674.6257	-672.7127	-670.6787	-672.2491
V	-503.6115	-502.6188	-503.5956	-675.0533	-674.0394	-675.0136	-673.1855	-671.5382	-673.1583
Zn	-493.9854	-491.5010	-493.9743	-664.9935	-663.0932	-664.9758	-663.7735	-661.8097	-663.7959
Ag	-494.4055	-492.4511	-494.3905	-664.6322	-662.9060	-664.6353	-664.3972	-662.3588	-665.0570
Cd	-493.3084	-491.1781	-493.2951	-663.8832	-661.6272	-663.8653	-661.8518	-659.9601	-661.8631
In	-498.5272	-496.6593	-498.5908	-666.3968	-663.7707	-666.3845	-663.6532	-661.5581	-663.6913
Mo	-504.5248	-503.3763	-504.5148	-675.3472	-674.7118	-675.4389	-674.7186	-672.9335	-674.7397
Nb	-505.3967	-504.7113	-505.3982	-676.0492	-674.1997	-675.4107	-674.6606	-672.8268	-674.5488
Pd	-500.0370	-498.3310	-500.0455	-669.0243	-667.0759	-669.0205	-669.1169	-667.3223	-669.1119
Rh	-499.2225	-497.3162	-499.2170	-672.7920	-670.7853	-672.8099	-671.4286	-670.3036	-671.4181
Ru	-503.9986	-502.1908	-503.9640	-674.0273	-672.4060	-674.0339	-672.9956	-672.1332	-672.9909
Sb	-497.3836	-495.1348	-497.3442	-666.7198	-664.9611	-666.7190	-666.8632	-664.8131	-666.8670
Sn	-499.4952	-497.2007	-499.1116	-667.1459	-665.3835	-667.0999	-665.9821	-663.8277	-665.9755
Tc	-503.0602	-501.1754	-503.0532	-674.4342	-673.8164	-674.4559	-674.0615	-672.9747	-674.0738
Y	-503.9232	-502.0670	-503.8988	-673.7620	-671.6132	-673.2241	-669.4633	-668.0403	-669.5030
Zr	-505.2907	-503.9148	-505.1817	-675.6874	-673.5456	-675.0519	-673.1694	-671.1993	-672.8072
Au	-497.0784	-495.1720	-497.0175	-665.1479	-663.3239	-665.1370	-666.4185	-664.2892	-666.5182
Bi	-496.9946	-494.7679	-496.9934	-665.9563	-664.2409	-666.0512	-665.0896	-663.2974	-665.0887
Hf	-506.4837	-504.9734	-506.4777	-677.3077	-675.1797	-676.6502	-674.7209	-672.6650	-674.2149
Hg	-491.0035	-488.7951	-490.9728	-661.2458	-659.2406	-661.2398	-661.7192	-659.8398	-661.7300
Ir	-503.0227	-501.1368	-503.0217	-673.9926	-672.0068	-674.0087	-673.5129	-672.6725	-673.4975
Os	-504.7648	-502.9878	-504.8105	-675.2098	-673.6653	-675.2235	-674.9483	-674.1970	-674.9223
Pb	-499.1183	-497.1173	-499.0544	-666.4446	-664.6897	-666.4625	-664.0200	-662.2222	-664.0123
Pt	-499.3356	-497.5110	-499.3215	-670.3996	-668.2412	-670.4147	-671.1408	-669.2725	-671.1370
Re	-504.1830	-502.4735	-504.1746	-675.7670	-675.0715	-675.7486	-675.8701	-674.9245	-675.8233
Ta	-506.6180	-505.7793	-506.6241	-677.7222	-675.9907	-677.0911	-676.4371	-674.5434	-676.4262
Tl	-497.9559	-496.1578	-497.9382	-664.5047	-662.7051	-664.5051	-662.6279	-660.6086	-662.6317
W	-505.8134	-504.9085	-505.8030	-676.5304	-676.1384	-676.9965	-676.7669	-675.4895	-676.7356

Note: Energies of the most stable configurations are highlighted in bold.

1.3 DFT energies and energy corrections

Table 2: Free energies at 298.15 K for isolated species.

Species	Free Energy (eV)
CO ₂	-23.3140
CO	-15.3336
CH ₄	-23.4639
H ₂	-6.9315
H ₂ O	-14.3239
COOH	-24.3963
CHO	-17.0983
CH ₂ O	-22.1607
OCH ₃	-24.5075
O	-1.9007
OH	-7.7303

Note: VASPKIT [10] was employed to calculate free energies.

1.4 Correlation analysis of adsorption energies

Figure 9 presents a Pearson correlation map that illustrates the relationships between the adsorption energies of various intermediates. This analysis encompasses all six substrates under consideration. The mean Pearson correlation coefficient is 0.6023 with a variance of 0.0109, signifying a robust correlation between the adsorption energies of different intermediates, accompanied by low variability.

1.5 The scaling relation scheme and the hybrid scaling relation

In line with the scaling relation framework proposed by Abild-Pedersen et al. [1], and later applied to the CO₂ reduction to methane process by Peterson & Nørskov [8], adsorbates in the CO₂RR process can be categorized into C-centered or O-centered species. In each group, a representative species is designated as the “descriptor”, allowing approximating the adsorption energies of other species within the same group using scaling relations. The following equations capture this relationship:

Table 3: Free energy corrections at 298.15 K for adsorbed intermediates.

Species	Free energy correction (eV)
*CO ₂	0.0864
*COOH	0.3693
*CO	0.0111
*CHO	0.2716
*CH ₂ O	0.5595
*OCH ₃	0.8738
*O	-0.0193
*OH	0.1993
*H	0.1533

Note: Free energy corrections were obtained by averaging the DFT-computed corrections, which include zero-point energy and entropy, across three substrates: g-C₃N₄, nitrogen-doped graphene, and dual-vacancy graphene.

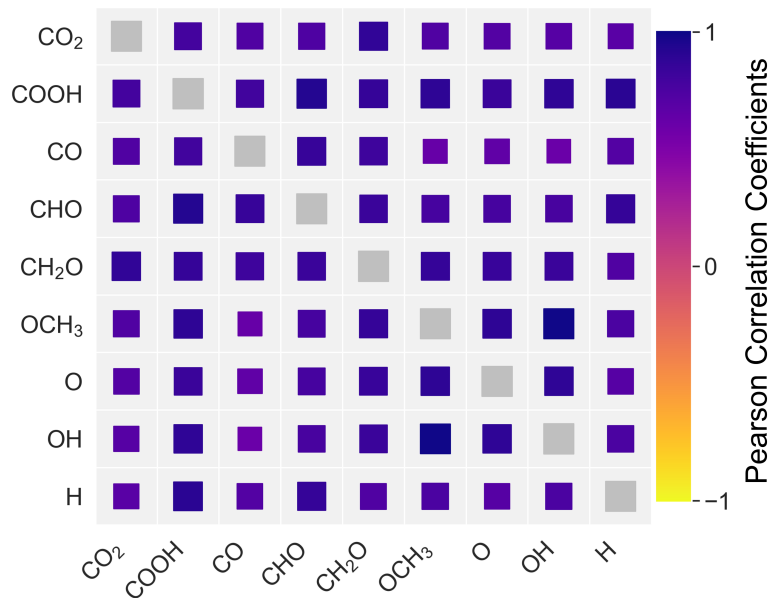


Figure 9: Pearson correlation map for adsorption energies of various adsorbates for all six substrates.

Table 4: DFT calculated final state energies in eV for adsorbates supported on g-C₃N₄.

Metal	*CO ₂	*COOH	*CO	*CHO	*CH ₂ O	*OCH ₃	*O	*OH	*H
Al	-481.2292	-504.7972	-508.6897	-496.4490	-500.7640	-503.7935	-509.9998	-488.6623	-485.4855
Co	-483.2039	-507.0765	-510.0453	-500.1329	-503.9316	-507.0552	-510.9052	-489.9487	-486.6194
Cr	-486.7813	-509.9599	-513.3962	-502.1493	-505.7125	-509.8851	-514.1702	-493.7457	-489.9202
Cu	-477.5955	-502.5914	-505.9613	-495.6511	-498.0502	-502.4590	-506.2829	-484.3166	-481.9683
Fe	-482.0576	-507.1508	-510.2918	-500.1101	-502.1626	-506.0115	-511.2543	-490.0116	-486.4067
Ga	-480.8854	-503.9317	-506.4938	-495.7379	-498.7813	-503.1345	-507.5029	-486.1702	-483.4575
Ge	-481.5807	-504.6467	-508.4204	-496.4421	-500.5712	-504.0218	-509.4116	-488.4168	-485.2680
Mn	-483.7690	-508.5410	-511.6514	-500.6279	-502.6739	-508.6433	-512.8569	-491.2239	-488.1082
Ni	-482.0061	-505.1988	-508.4173	-498.5054	-501.0040	-504.8945	-508.6266	-487.3684	-484.8272
Sc	-483.9963	-509.3147	-512.9882	-501.4505	-505.2024	-509.4054	-514.5969	-493.4105	-489.2632
Ti	-484.2282	-509.6510	-512.8528	-502.0410	-505.3761	-509.9729	-514.0700	-493.6478	-489.2234
V	-484.1990	-508.6926	-512.3009	-501.6777	-504.4297	-509.3618	-513.4561	-493.8569	-488.9474
Zn	-475.2375	-500.3556	-504.4103	-492.4144	-496.5426	-499.4232	-504.6297	-482.6782	-481.0438
Ag	-476.7049	-501.6430	-504.5861	-493.9138	-496.7220	-500.9477	-504.5408	-482.6604	-481.2659
Cd	-475.1288	-500.1854	-503.4108	-491.8954	-495.6486	-499.4959	-503.6209	-483.3427	-479.8278
In	-481.1330	-504.1653	-506.4422	-496.0016	-498.6643	-503.3286	-507.3780	-485.6281	-483.1445
Mo	-484.2892	-509.4263	-512.9103	-503.0025	-505.5534	-509.6730	-513.0136	-493.5700	-489.4994
Nb	-485.4055	-510.7952	-514.0380	-503.5663	-506.3671	-511.1572	-514.7845	-495.5118	-490.2111
Pd	-481.5399	-504.7593	-508.5173	-498.0817	-501.1620	-504.0892	-508.1976	-486.1551	-483.9553
Rh	-479.8884	-505.2422	-508.6754	-498.7129	-501.4594	-504.5254	-508.9536	-487.8771	-485.0738
Ru	-483.8526	-507.5120	-511.5881	-500.6857	-504.1497	-506.8934	-510.9524	-490.6690	-488.0169
Sb	-478.5169	-502.9708	-506.5211	-494.8740	-498.9453	-502.5347	-507.2111	-486.4448	-483.4418
Sn	-481.4238	-504.4677	-507.8470	-496.2883	-499.9258	-503.6685	-508.8152	-487.6963	-484.6351
Tc	-482.7091	-507.9652	-512.1064	-501.9896	-504.6034	-508.3486	-511.4777	-492.0381	-488.0897
Y	-484.6612	-509.8564	-513.6851	-501.9522	-505.8238	-509.8344	-515.2400	-493.4038	-489.6506
Zr	-485.4694	-511.1852	-514.3901	-503.1958	-506.9346	-511.5864	-515.6720	-496.3037	-490.4785
Au	-479.1941	-502.3245	-506.9013	-495.6782	-499.0711	-501.6877	-506.5462	-484.6198	-483.6909
Bi	-478.2695	-502.8490	-506.2055	-494.6965	-498.5557	-502.3398	-506.7999	-485.7536	-483.1348
Hf	-486.5155	-512.4535	-515.5965	-504.3393	-508.1599	-512.8332	-517.2187	-496.4195	-491.7486
Hg	-472.8730	-500.0491	-502.1889	-491.7544	-494.1224	-499.2181	-501.8365	-480.3761	-479.2046
Ir	-483.7878	-507.2024	-510.6763	-500.2051	-503.2948	-506.5209	-509.8509	-490.9790	-487.3503
Os	-484.9279	-508.6427	-512.5954	-501.8541	-505.2080	-507.8334	-511.8734	-491.0155	-489.0898
Pb	-481.3587	-504.4450	-507.5634	-496.2379	-499.6114	-503.5822	-508.1698	-486.8476	-484.2646
Pt	-481.1676	-504.3670	-508.2170	-499.0073	-500.9446	-504.2695	-508.1465	-487.3508	-484.6644
Re	-483.6421	-508.9474	-512.8388	-502.8952	-505.3651	-509.1168	-512.6374	-493.0621	-489.2811
Ta	-486.3299	-512.1371	-515.1895	-504.6585	-507.5888	-512.5295	-516.0165	-497.0134	-490.5695
Tl	-480.7357	-503.7632	-505.9937	-495.5894	-497.7724	-503.0564	-506.7919	-484.0732	-482.3846
W	-485.2596	-510.8145	-514.28	-504.2714	-506.7988	-511.0643	-514.2358	-494.4330	-490.6506

Table 5: DFT calculated final state energies in eV for adsorbates supported on nitrogen-doped graphene.

Metal	*CO ₂	*COOH	*CO	*CHO	*CH ₂ O	*OCH ₃	*O	*OH	*H
Al	-652.7589	-675.7997	-679.7595	-668.0296	-671.7596	-676.2161	-681.1311	-658.7849	-656.4702
Co	-654.3280	-677.5394	-681.2518	-670.0860	-673.9208	-676.7761	-680.7219	-659.1714	-657.8777
Cr	-657.0479	-680.2074	-683.7982	-673.0760	-676.1859	-679.4701	-684.5295	-664.7306	-660.4141
Cu	-650.2181	-673.3928	-675.5873	-665.2174	-668.0662	-672.5797	-675.7047	-653.5770	-652.1010
Fe	-655.4034	-678.5897	-682.1186	-671.9101	-674.7438	-677.8515	-682.1216	-661.5422	-658.7383
Ga	-649.9563	-672.9807	-676.9763	-664.9727	-669.0739	-672.8536	-677.7169	-655.5345	-653.9243
Ge	-651.0391	-674.1655	-677.2582	-665.9255	-669.5282	-673.3438	-678.1585	-657.4964	-654.3444
Mn	-656.5635	-679.7128	-683.1092	-672.6753	-675.6877	-679.0710	-683.3898	-663.1584	-659.7760
Ni	-653.1461	-676.3270	-678.5166	-668.1448	-671.1502	-675.5454	-678.5411	-656.3929	-655.1238
Sc	-655.2274	-678.9985	-682.8810	-670.9489	-674.9850	-679.1986	-684.3192	-662.2442	-659.0243
Ti	-655.5937	-680.2412	-683.5514	-671.9689	-675.9724	-680.4589	-685.1366	-665.2871	-659.7132
V	-656.0751	-680.2584	-683.5739	-672.6281	-676.0229	-680.5926	-684.9400	-665.6038	-659.9017
Zn	-648.2316	-671.3824	-674.1973	-663.2623	-666.3990	-670.5613	-674.5436	-652.2900	-650.9227
Ag	-646.9759	-670.2666	-673.2766	-663.1058	-665.7601	-669.7801	-673.0113	-651.0760	-649.9287
Cd	-646.1687	-669.2620	-672.8043	-661.4439	-664.9473	-668.8180	-672.9588	-650.7684	-649.7670
In	-648.6726	-671.7218	-675.3788	-663.4885	-667.5183	-670.7536	-675.8630	-653.8535	-652.4757
Mo	-655.7944	-680.2966	-683.6262	-672.7667	-676.3955	-680.6291	-684.8234	-665.8138	-659.8169
Nb	-656.0277	-680.8814	-684.2662	-672.5576	-676.9139	-681.4203	-685.7720	-666.2363	-660.3734
Pd	-652.2091	-675.3967	-677.2760	-667.1855	-669.8609	-674.6033	-677.3498	-655.1080	-654.0027
Rh	-653.6928	-676.9529	-680.9755	-669.5137	-673.6394	-676.2879	-680.2104	-658.6953	-657.6908
Ru	-654.5425	-678.2124	-681.9561	-672.0589	-674.6177	-678.0945	-681.9008	-661.3838	-658.6572
Sb	-649.9262	-672.9182	-675.6457	-664.7128	-667.9159	-672.0849	-675.8420	-655.1699	-652.4240
Sn	-650.5072	-673.6118	-675.7767	-665.3842	-668.0544	-672.7597	-676.5046	-655.8947	-652.9261
Tc	-655.4025	-679.3044	-682.7454	-672.5785	-676.3294	-679.4840	-683.3209	-664.2323	-659.2703
Y	-655.2660	-679.0430	-682.7571	-670.8208	-674.7780	-679.0775	-684.1210	-661.8034	-658.8885
Zr	-655.9118	-680.6859	-684.1920	-672.1497	-676.4014	-680.7930	-685.7940	-665.4878	-660.4163
Au	-648.3344	-671.3969	-673.1469	-663.1955	-665.5964	-670.5800	-673.6092	-651.2436	-649.7275
Bi	-649.1484	-672.1225	-675.1630	-663.9594	-667.2981	-671.4617	-675.6926	-654.7684	-651.8907
Hf	-657.3364	-682.3019	-685.8119	-673.6603	-678.0090	-682.4001	-687.4607	-666.9550	-662.0651
Hg	-644.7368	-667.9224	-671.2200	-659.6906	-663.5208	-667.0466	-670.9016	-648.8944	-648.3755
Ir	-654.8564	-678.1079	-682.2865	-670.9826	-674.9484	-677.4097	-681.3088	-660.1543	-658.9895
Os	-655.6722	-679.5364	-683.3240	-673.4289	-675.9254	-679.4423	-683.1300	-663.0791	-659.9901
Pb	-649.8843	-672.9588	-674.5856	-664.7553	-667.1174	-672.0886	-675.8823	-653.6827	-651.5940
Pt	-653.3281	-676.5221	-678.6094	-668.2951	-671.2463	-675.7317	-678.4334	-656.4419	-655.4733
Re	-656.3492	-680.7664	-683.9596	-673.9732	-676.5164	-681.0627	-684.8096	-665.9526	-660.5620
Ta	-657.1988	-682.6048	-685.8231	-674.1666	-678.5029	-682.9709	-687.2294	-667.7321	-661.8794
Tl	-648.1346	-671.1831	-673.2953	-662.9610	-665.6240	-670.3512	-673.4567	-651.7909	-650.4750
W	-657.0204	-682.0186	-685.3735	-674.3843	-678.2483	-682.4377	-686.3613	-667.4547	-661.5686

Table 6: DFT calculated final state energies in eV for adsorbates supported on graphene with dual-vacancy.

Metal	*CO ₂	*COOH	*CO	*CHO	*CH ₂ O	*OCH ₃	*O	*OH	*H
Al	-650.3496	-673.3468	-676.2273	-665.6303	-668.4112	-672.5763	-677.4453	-655.0864	-653.0166
Co	-652.5157	-675.5864	-679.3861	-669.0614	-672.8955	-675.8508	-679.5268	-658.7929	-655.9377
Cr	-655.0421	-678.1256	-681.8470	-671.1282	-674.2868	-679.1554	-683.4111	-663.3554	-658.4913
Cu	-649.8187	-672.9161	-674.9327	-664.8190	-669.0819	-672.1515	-674.7438	-652.8789	-653.6953
Fe	-653.7964	-677.0127	-680.3412	-670.0219	-673.9525	-676.7631	-681.1346	-660.9239	-656.9759
Ga	-649.0340	-672.0433	-674.9630	-663.8505	-667.2101	-671.2541	-675.5229	-653.2086	-651.8693
Ge	-651.0133	-674.2532	-677.2272	-666.0554	-669.5660	-673.4485	-677.8152	-655.7843	-654.2731
Mn	-654.8183	-678.0584	-681.5834	-670.9593	-674.0994	-677.9260	-682.6048	-662.5702	-658.1064
Ni	-651.5295	-674.6692	-677.8941	-667.2937	-670.7325	-673.9392	-677.5204	-656.1026	-655.6559
Sc	-652.1630	-675.5777	-678.6101	-667.5024	-670.7255	-675.4361	-680.0287	-658.0834	-654.6913
Ti	-654.2548	-677.9326	-681.1516	-670.0780	-673.2830	-677.9113	-682.6933	-661.1957	-657.4040
V	-654.6939	-678.0200	-681.8606	-670.8517	-674.2298	-679.2097	-683.4928	-663.1639	-658.4619
Zn	-646.9805	-670.1676	-672.2508	-662.0849	-664.7199	-669.3791	-672.6028	-650.3134	-648.8961
Ag	-647.4840	-670.5954	-672.4765	-662.3757	-665.1014	-669.8199	-672.2893	-650.2207	-651.5223
Cd	-645.2038	-668.3897	-670.2685	-660.2502	-662.7479	-667.5994	-670.6023	-648.2958	-646.9658
In	-646.8189	-669.9379	-673.1820	-661.7351	-665.3833	-669.1524	-673.5557	-651.3730	-650.2004
Mo	-656.2058	-679.7202	-683.2424	-672.3832	-675.6459	-679.9903	-684.8002	-664.6331	-659.9673
Nb	-656.1010	-679.4842	-683.3623	-672.0587	-675.6683	-679.5996	-684.8935	-664.2634	-659.9617
Pd	-650.5405	-673.6524	-677.0119	-666.0816	-669.7529	-672.9394	-676.5341	-655.1586	-654.8764
Rh	-652.7998	-675.8992	-679.6974	-669.1468	-672.2062	-676.2142	-679.9592	-659.4214	-656.7388
Ru	-654.8166	-678.0140	-681.6090	-671.1415	-674.0502	-677.9828	-682.4415	-662.4653	-658.2092
Sb	-649.9882	-673.0639	-675.9906	-664.8414	-668.3621	-672.2685	-676.6274	-655.1055	-653.1345
Sn	-648.5997	-671.7246	-675.2765	-663.7120	-667.5399	-670.8850	-675.8484	-653.8138	-652.4041
Tc	-655.8173	-679.2476	-682.6345	-672.1709	-675.0076	-679.2729	-683.7569	-664.1434	-659.2908
Y	-652.1517	-675.4891	-678.6682	-667.4644	-670.6934	-675.1478	-680.0013	-658.3045	-654.7163
Zr	-654.8760	-678.4572	-681.6839	-670.6090	-673.8291	-678.4537	-683.1390	-661.4741	-657.9892
Au	-649.3963	-672.5116	-674.3660	-664.2836	-667.3357	-671.7273	-674.1359	-652.0358	-653.1138
Bi	-648.8651	-672.0004	-673.7920	-663.7934	-666.2170	-671.1801	-674.0672	-652.8628	-650.9149
Hf	-656.1155	-679.7805	-683.2130	-671.9925	-675.3123	-679.9256	-684.7502	-662.8630	-659.4860
Hg	-645.0948	-668.2801	-669.9749	-660.1062	-662.5696	-667.4822	-670.2672	-647.8582	-646.7652
Ir	-654.4999	-677.8310	-681.7312	-671.1936	-674.7821	-678.1749	-681.9532	-661.9662	-658.5262
Os	-656.3635	-679.8433	-683.4557	-673.1036	-675.9479	-679.6710	-684.4704	-664.7281	-660.0873
Pb	-647.8007	-670.9491	-673.2996	-662.7392	-665.6502	-670.1373	-673.5969	-651.6692	-650.4432
Pt	-652.4961	-675.6092	-678.9183	-668.2053	-671.6867	-674.8876	-678.4355	-657.4936	-656.2759
Re	-657.2440	-681.0777	-684.5183	-673.9603	-676.8950	-681.2383	-685.8328	-666.1615	-661.2885
Ta	-657.4068	-681.0711	-685.1062	-673.5947	-677.3738	-681.6985	-686.7561	-666.0327	-661.7361
Tl	-645.7286	-668.8734	-671.7205	-660.7259	-664.0001	-668.1110	-672.0305	-649.7198	-648.7563
W	-657.5901	-681.6722	-685.1010	-674.1028	-677.7828	-682.4493	-686.6385	-666.9364	-661.8641

Table 7: Zero-point energies in eV for relaxed adsorbates supported on g-C₃N₄ at 298.15 K.

Metal	*CO ₂	*COOH	*CO	*CHO	*CH ₂ O	*OCH ₃	*O	*OH	*H
Al	0.2905	0.6130	0.1743	0.4606	0.7456	1.0974	0.0629	0.3521	0.1925
Co	0.3038	0.5895	0.2051	0.4186	0.6269	1.0663	0.0571	0.3248	0.1507
Cr	0.3140	0.5964	0.1640	0.4374	0.7725	1.0779	0.0670	0.3286	0.1626
Cu	0.3157	0.6016	0.2045	0.4498	0.7797	1.0751	0.0494	0.3332	0.1577
Fe	0.3088	0.5859	0.1931	0.4437	0.7720	1.0726	0.0599	0.3326	0.1550
Ga	0.3102	0.6131	0.1448	0.4665	0.7186	1.0680	0.0608	0.3202	0.1813
Ge	0.3091	0.6069	0.1396	0.4540	0.7269	1.0881	0.0581	0.3506	0.1904
Mn	0.3022	0.5876	0.1733	0.4333	0.7637	1.0622	0.0687	0.3219	0.1432
Ni	0.3023	0.5934	0.2074	0.4546	0.7662	1.0623	0.0542	0.3313	0.1611
Sc	0.2880	0.6039	0.1771	0.4544	0.7473	1.0806	0.0657	0.3156	0.1480
Ti	0.3044	0.6088	0.1889	0.4664	0.7863	1.0862	0.0796	0.3417	0.1590
V	0.3081	0.6005	0.2031	0.4408	0.7868	1.0882	0.0792	0.3388	0.1660
Zn	0.3243	0.6080	0.1729	0.4601	0.7277	1.0832	0.0514	0.3468	0.1726
Ag	0.3167	0.5993	0.1815	0.4457	0.7264	1.0590	0.0390	0.3304	0.1576
Cd	0.3242	0.6007	0.1533	0.4502	0.7292	1.0604	0.0983	0.3322	0.1439
In	0.3116	0.5687	0.1399	0.4025	0.7158	1.0551	0.0523	0.3315	0.1141
Mo	0.3109	0.6071	0.2163	0.4441	0.7970	1.0825	0.0765	0.3312	0.1851
Nb	0.3101	0.5971	0.2013	0.4340	0.7960	1.0908	0.0798	0.3329	0.1598
Pd	0.3148	0.6091	0.1996	0.4778	0.7402	1.0777	0.0525	0.3425	0.1508
Rh	0.3064	0.6180	0.2215	0.4654	0.7649	1.0844	0.0615	0.3643	0.1946
Ru	0.3060	0.6201	0.2104	0.4668	0.7761	1.0800	0.0663	0.3421	0.2026
Sb	0.3050	0.6244	0.1461	0.4696	0.7473	1.1052	0.0689	0.3676	0.2043
Sn	0.3115	0.5941	0.1441	0.4373	0.7202	1.0761	0.0591	0.3397	0.1601
Tc	0.3170	0.6102	0.2178	0.4543	0.7890	1.0807	0.0698	0.3442	0.2008
Y	0.2768	0.5949	0.1712	0.4467	0.7278	1.0780	0.0573	0.3206	0.1349
Zr	0.2939	0.6068	0.1888	0.4631	0.7737	1.0875	0.0744	0.3155	0.1592
Au	0.3123	0.6245	0.2147	0.4761	0.7312	1.0845	0.0527	0.3432	0.2066
Bi	0.3076	0.6148	0.1485	0.4612	0.7392	1.0935	0.0611	0.3554	0.1893
Hf	0.2928	0.6104	0.1880	0.4658	0.7769	1.0954	0.0765	0.3218	0.1728
Hg	0.3220	0.6221	0.1486	0.4707	0.7338	1.0809	0.0541	0.3469	0.1924
Ir	0.3127	0.6311	0.2271	0.4818	0.7530	1.0740	0.1084	0.3314	0.2142
Os	0.3122	0.6260	0.2258	0.4796	0.7531	1.0911	0.0670	0.3501	0.2154
Pb	0.3152	0.5834	0.1401	0.4239	0.7113	1.0486	0.0513	0.3043	0.1352
Pt	0.3144	0.6361	0.2225	0.4908	0.7569	1.0921	0.0603	0.3672	0.2058
Re	0.3171	0.6175	0.2213	0.4665	0.8021	1.0985	0.0780	0.3597	0.2032
Ta	0.3099	0.5977	0.2000	0.4414	0.7993	1.0880	0.0847	0.3410	0.1780
Tl	0.3114	0.5614	0.1389	0.3494	0.7105	1.0410	0.0246	0.3210	0.0951
W	0.3146	0.6059	0.2160	0.4456	0.8033	1.0886	0.0725	0.3387	0.1834

Table 8: Entropy corrections ($-T \cdot S$) in eV for relaxed adsorbates supported on g-C₃N₄ at 298.15 K.

Metal	*CO ₂	*COOH	*CO	*CHO	*CH ₂ O	*OCH ₃	*O	*OH	*H
Al	-0.2195	-0.2476	-0.1874	-0.1939	-0.2359	-0.1759	-0.0894	-0.1010	-0.0124
Co	-0.2359	-0.2665	-0.1544	-0.1572	-0.1755	-0.2095	-0.1078	-0.1510	-0.0341
Cr	-0.1862	-0.2605	-0.2075	-0.2069	-0.1478	-0.1733	-0.0790	-0.1437	-0.0221
Cu	-0.3098	-0.2403	-0.1655	-0.1803	-0.1647	-0.2378	-0.0977	-0.1375	-0.0297
Fe	-0.2184	-0.2028	-0.1676	-0.1797	-0.1742	-0.2640	-0.0815	-0.1285	-0.0215
Ga	-0.2602	-0.2558	-0.2291	-0.1881	-0.1252	-0.2576	-0.0897	-0.1441	-0.0182
Ge	-0.1978	-0.2423	-0.1635	-0.1802	-0.2104	-0.2364	-0.1178	-0.1052	-0.0087
Mn	-0.2142	-0.2678	-0.1863	-0.2059	-0.1788	-0.2752	-0.0808	-0.1425	-0.0261
Ni	-0.2460	-0.1948	-0.1592	-0.1224	-0.1275	-0.2506	-0.0997	-0.1384	-0.0224
Sc	-0.2227	-0.2369	-0.1843	-0.1667	-0.1817	-0.2035	-0.0728	-0.1416	-0.0226
Ti	-0.1978	-0.2263	-0.1685	-0.1389	-0.1414	-0.1795	-0.0578	-0.1013	-0.0195
V	-0.2603	-0.2511	-0.1452	-0.2028	-0.1360	-0.2374	-0.0612	-0.1082	-0.0186
Zn	-0.2928	-0.2543	-0.1909	-0.1959	-0.2202	-0.2331	-0.0910	-0.1185	-0.0228
Ag	-0.2458	-0.2428	-0.1910	-0.1890	-0.3097	-0.2421	-0.1060	-0.1392	-0.0276
Cd	-0.2961	-0.2561	-0.2368	-0.2023	-0.2076	-0.2630	-0.0270	-0.1408	-0.0337
In	-0.1978	-0.2895	-0.1071	-0.1840	-0.1338	-0.2826	-0.1011	-0.1386	-0.0405
Mo	-0.1912	-0.2310	-0.1310	-0.1680	-0.1269	-0.2228	-0.0641	-0.1496	-0.0155
Nb	-0.1896	-0.2540	-0.1460	-0.1924	-0.1290	-0.2147	-0.0575	-0.1177	-0.0261
Pd	-0.2405	-0.2385	-0.1649	-0.1740	-0.2538	-0.2201	-0.0900	-0.1143	-0.0518
Rh	-0.2408	-0.2385	-0.1355	-0.1734	-0.1853	-0.2247	-0.0863	-0.0866	-0.0222
Ru	-0.2197	-0.2304	-0.1450	-0.1769	-0.1655	-0.1574	-0.0832	-0.1294	-0.0138
Sb	-0.2354	-0.2277	-0.1320	-0.1793	-0.2211	-0.1961	-0.0616	-0.0808	-0.0090
Sn	-0.2606	-0.2544	-0.2227	-0.2021	-0.3045	-0.2568	-0.0787	-0.1171	-0.0160
Tc	-0.1875	-0.2373	-0.1347	-0.1733	-0.1485	-0.2301	-0.0697	-0.1007	-0.0121
Y	-0.2557	-0.2528	-0.1929	-0.1886	-0.2130	-0.2081	-0.0824	-0.1393	-0.0285
Zr	-0.2083	-0.2325	-0.1624	-0.1459	-0.1574	-0.2014	-0.0640	-0.1556	-0.0208
Au	-0.1901	-0.2267	-0.1484	-0.1846	-0.2939	-0.2307	-0.0857	-0.1271	-0.0138
Bi	-0.2366	-0.2392	-0.1915	-0.1899	-0.2361	-0.1986	-0.0683	-0.0934	-0.0100
Hf	-0.2043	-0.2219	-0.1618	-0.1418	-0.1489	-0.1981	-0.0610	-0.1414	-0.0163
Hg	-0.2980	-0.2371	-0.2812	-0.1995	-0.3039	-0.2465	-0.0878	-0.1245	-0.0175
Ir	-0.2097	-0.2290	-0.1261	-0.1803	-0.1913	-0.2221	-0.0377	-0.1379	-0.0159
Os	-0.1795	-0.2235	-0.1294	-0.1519	-0.1609	-0.2027	-0.0680	-0.1093	-0.0124
Pb	-0.2546	-0.2691	-0.1666	-0.2165	-0.2641	-0.2520	-0.1007	-0.1097	-0.0257
Pt	-0.2411	-0.2029	-0.1496	-0.1593	-0.2009	-0.2246	-0.0950	-0.0937	-0.0137
Re	-0.1869	-0.2262	-0.1293	-0.1697	-0.1266	-0.2165	-0.0644	-0.0953	-0.0146
Ta	-0.1872	-0.2532	-0.1523	-0.1847	-0.1265	-0.1798	-0.0535	-0.1040	-0.0177
Tl	-0.2599	-0.2833	-0.1807	-0.1538	-0.2422	-0.1501	-0.0126	-0.1338	-0.0533
W	-0.1791	-0.2368	-0.1335	-0.1723	-0.1225	-0.2253	-0.0673	-0.1180	-0.0201

Table 9: Zero-point energies in eV for relaxed adsorbates supported on nitrogen-doped graphene at 298.15 K.

Metal	*CO ₂	*COOH	*CO	*CHO	*CH ₂ O	*OCH ₃	*O	*OH	*H
Al	0.3093	0.6024	0.1683	0.4395	0.7509	1.0855	0.0552	0.3401	0.1864
Co	0.3140	0.6247	0.2044	0.4787	0.7345	1.0615	0.0606	0.3315	0.2006
Cr	0.3108	0.5983	0.2007	0.4410	0.7211	1.0824	0.0828	0.3253	0.1625
Cu	0.3145	0.5943	0.1460	0.4377	0.7196	1.0160	0.0407	0.3104	0.1523
Fe	0.3117	0.6148	0.2195	0.4634	0.7877	1.0678	0.0703	0.3163	0.1858
Ga	0.3129	0.6080	0.1561	0.4537	0.7495	1.0826	0.0573	0.3420	0.1897
Ge	0.3131	0.6206	0.1402	0.4629	0.7281	1.1014	0.0686	0.3538	0.2110
Mn	0.3120	0.6111	0.2128	0.4601	0.8078	1.0640	0.0793	0.3148	0.2040
Ni	0.3110	0.6059	0.1485	0.4602	0.7283	1.0467	0.0402	0.3168	0.1620
Sc	0.2741	0.5910	0.1620	0.4456	0.7019	1.0758	0.0575	0.3166	0.1338
Ti	0.2920	0.6020	0.1781	0.4525	0.7593	1.0831	0.0731	0.2981	0.1481
V	0.2984	0.6055	0.1865	0.4609	0.7756	1.0843	0.0786	0.3171	0.1525
Zn	0.3143	0.5928	0.1554	0.4357	0.7116	1.0521	0.0394	0.3248	0.1640
Ag	0.3127	0.5862	0.1862	0.4307	0.7518	1.0419	0.0356	0.3231	0.1308
Cd	0.3055	0.5910	0.1518	0.4402	0.7312	1.0524	0.0366	0.3189	0.1483
In	0.3096	0.5986	0.1414	0.4477	0.7152	1.0724	0.0437	0.3300	0.1609
Mo	0.2949	0.6111	0.1914	0.4728	0.7806	1.0887	0.0795	0.3253	0.1500
Nb	0.2946	0.5996	0.1767	0.4601	0.7874	1.0896	0.0742	0.3048	0.1515
Pd	0.3122	0.5993	0.1444	0.4490	0.7303	1.0342	0.0300	0.3047	0.1558
Rh	0.3115	0.6288	0.1969	0.4826	0.7388	1.0867	0.0602	0.3453	0.2025
Ru	0.3152	0.6122	0.2180	0.4569	0.7918	1.0947	0.0698	0.3483	0.1873
Sb	0.3115	0.5874	0.1397	0.4349	0.7184	1.0467	0.0646	0.3351	0.1752
Sn	0.3112	0.6002	0.1400	0.4367	0.7239	1.0836	0.0568	0.3359	0.1710
Tc	0.3053	0.6110	0.2105	0.4251	0.7934	1.0870	0.0807	0.3496	0.1741
Y	0.2709	0.5835	0.1580	0.4307	0.7059	1.0703	0.0500	0.3200	0.1226
Zr	0.2719	0.5963	0.1723	0.4430	0.7327	1.0846	0.0669	0.3176	0.1472
Au	0.3137	0.5480	0.1442	0.3577	0.7209	0.9864	0.0174	0.2881	0.1027
Bi	0.3111	0.5778	0.1378	0.4190	0.7133	1.0475	0.0550	0.3241	0.1533
Hf	0.2699	0.6002	0.1714	0.4452	0.7372	1.0904	0.0687	0.3242	0.1569
Hg	0.3113	0.6082	0.1397	0.4569	0.7258	1.0720	0.0412	0.3304	0.1625
Ir	0.3132	0.6309	0.2106	0.4856	0.7390	1.0888	0.0626	0.3456	0.2022
Os	0.3156	0.6148	0.2179	0.4592	0.7971	1.0984	0.0768	0.3463	0.1812
Pb	0.3116	0.5352	0.1385	0.3677	0.7147	1.0532	0.0474	0.3172	0.1302
Pt	0.3139	0.6134	0.1439	0.4671	0.7359	1.0406	0.0482	0.3114	0.1736
Re	0.3035	0.6045	0.2095	0.4566	0.7995	1.0957	0.0846	0.3493	0.1818
Ta	0.2751	0.6019	0.1869	0.4630	0.7724	1.0937	0.0751	0.3060	0.1669
Tl	0.3131	0.5988	0.1402	0.4439	0.7193	1.0169	0.0573	0.3244	0.1506
W	0.2889	0.6117	0.1927	0.4777	0.7852	1.0941	0.0810	0.3273	0.1832

Table 10: Entropy corrections ($-T \cdot S$) in eV for relaxed adsorbates supported on nitrogen-doped graphene at 298.15 K.

Metal	*CO ₂	*COOH	*CO	*CHO	*CH ₂ O	*OCH ₃	*O	*OH	*H
Al	-0.1981	-0.2564	-0.1979	-0.1424	-0.2051	-0.1839	-0.0794	-0.1211	-0.0113
Co	-0.2358	-0.2213	-0.1589	-0.1584	-0.2025	-0.2223	-0.0701	-0.0817	-0.0123
Cr	-0.2593	-0.1973	-0.1568	-0.2037	-0.2291	-0.1679	-0.0569	-0.0875	-0.0228
Cu	-0.2457	-0.2636	-0.2132	-0.2040	-0.1267	-0.2137	-0.1188	-0.1711	-0.0226
Fe	-0.1936	-0.2385	-0.1356	-0.1758	-0.1985	-0.1910	-0.0647	-0.0892	-0.0172
Ga	-0.2565	-0.1937	-0.1600	-0.2025	-0.2139	-0.1766	-0.0727	-0.1269	-0.0126
Ge	-0.2469	-0.2413	-0.1027	-0.1937	-0.1687	-0.1551	-0.0690	-0.1091	-0.0080
Mn	-0.1929	-0.2402	-0.1409	-0.1736	-0.1949	-0.2011	-0.0563	-0.1631	-0.0160
Ni	-0.1239	-0.2440	-0.2027	-0.1785	-0.2318	-0.1792	-0.0929	-0.1520	-0.0170
Sc	-0.1938	-0.2647	-0.1418	-0.2024	-0.2291	-0.2139	-0.0790	-0.1516	-0.0293
Ti	-0.2093	-0.2423	-0.1798	-0.1640	-0.1765	-0.1433	-0.0692	-0.1462	-0.0262
V	-0.2112	-0.2373	-0.1734	-0.1578	-0.1642	-0.0767	-0.0621	-0.1522	-0.0273
Zn	-0.2567	-0.2001	-0.2491	-0.2135	-0.1581	-0.1396	-0.1091	-0.1668	-0.0211
Ag	-0.2600	-0.2035	-0.1802	-0.2231	-0.1723	-0.1531	-0.1293	-0.1487	-0.0596
Cd	-0.2615	-0.2042	-0.1827	-0.2185	-0.2727	-0.2094	-0.1192	-0.1850	-0.0320
In	-0.1886	-0.2021	-0.1593	-0.2221	-0.1949	-0.2061	-0.1158	-0.1603	-0.0238
Mo	-0.2049	-0.2075	-0.1659	-0.1327	-0.1650	-0.2041	-0.0605	-0.1258	-0.0437
Nb	-0.2072	-0.2300	-0.1145	-0.1439	-0.1403	-0.2086	-0.0684	-0.1863	-0.0251
Pd	-0.1843	-0.2620	-0.1476	-0.2000	-0.1645	-0.2057	-0.1131	-0.1688	-0.0223
Rh	-0.2986	-0.2220	-0.1669	-0.1667	-0.1953	-0.1423	-0.0693	-0.1229	-0.0149
Ru	-0.1998	-0.1779	-0.1375	-0.1827	-0.1455	-0.2017	-0.0653	-0.1103	-0.0202
Sb	-0.1938	-0.1984	-0.1084	-0.2024	-0.1970	-0.0996	-0.0780	-0.1183	-0.0109
Sn	-0.1931	-0.2040	-0.1708	-0.2214	-0.1801	-0.2006	-0.0911	-0.1474	-0.0185
Tc	-0.2038	-0.2277	-0.1483	-0.1505	-0.1515	-0.1810	-0.0569	-0.1008	-0.0234
Y	-0.1994	-0.2704	-0.1507	-0.1605	-0.2919	-0.2162	-0.0981	-0.1548	-0.0344
Zr	-0.2233	-0.2608	-0.1845	-0.1849	-0.2016	-0.2144	-0.0776	-0.1500	-0.0242
Au	-0.1872	-0.1923	-0.2237	-0.1738	-0.1907	-0.2639	-0.1497	-0.1276	-0.0301
Bi	-0.1978	-0.2736	-0.1731	-0.1581	-0.2369	-0.0995	-0.0937	-0.1386	-0.0171
Hf	-0.2235	-0.2562	-0.1836	-0.1839	-0.1987	-0.2082	-0.0759	-0.1417	-0.0211
Hg	-0.1907	-0.1929	-0.1053	-0.0955	-0.1765	-0.2558	-0.1157	-0.1694	-0.0357
Ir	-0.2967	-0.2218	-0.1486	-0.1659	-0.2038	-0.2134	-0.0723	-0.1326	-0.0200
Os	-0.1948	-0.2462	-0.1422	-0.1945	-0.1448	-0.2046	-0.0598	-0.1205	-0.0322
Pb	-0.1979	-0.2320	-0.1108	-0.2414	-0.1437	-0.2639	-0.1126	-0.1465	-0.0238
Pt	-0.1770	-0.2479	-0.1481	-0.1915	-0.2820	-0.2030	-0.0791	-0.1666	-0.0228
Re	-0.1958	-0.2535	-0.1508	-0.1867	-0.1462	-0.2483	-0.0561	-0.1018	-0.0249
Ta	-0.2078	-0.2197	-0.1675	-0.1373	-0.1542	-0.2084	-0.0698	-0.1979	-0.0195
Tl	-0.2573	-0.2043	-0.1719	-0.2270	-0.1288	-0.2326	-0.0688	-0.1876	-0.0332
W	-0.2007	-0.2007	-0.1642	-0.1194	-0.1565	-0.2032	-0.0607	-0.1275	-0.0202

Table 11: Zero-point energies in eV for relaxed adsorbates supported on graphene with dual-vacancy at 298.15 K.

Metal	*CO ₂	*COOH	*CO	*CHO	*CH ₂ O	*OCH ₃	*O	*OH	*H
Al	0.3140	0.5988	0.1888	0.4386	0.7218	1.0769	0.0472	0.3366	0.1729
Co	0.3080	0.6179	0.2173	0.4899	0.7928	1.0616	0.0573	0.3458	0.1726
Cr	0.3318	0.5862	0.1957	0.4277	0.8826	1.0733	0.0792	0.3294	0.1560
Cu	0.3140	0.6023	0.1769	0.5229	0.7172	1.0131	0.0323	0.3298	0.2857
Fe	0.3177	0.6110	0.2083	0.5038	0.7828	1.0802	0.0776	0.3515	0.1987
Ga	0.3126	0.6056	0.1492	0.4494	0.7196	1.0788	0.0446	0.3370	0.1810
Ge	0.3138	0.6171	0.1471	0.4657	0.7196	1.0935	0.0540	0.3514	0.2028
Mn	0.3167	0.6141	0.2050	0.4803	0.8009	1.0809	0.0756	0.3411	0.1594
Ni	0.3134	0.6251	0.1942	0.4571	0.7230	1.0738	0.0496	0.3521	0.2877
Sc	0.3229	0.5874	0.1668	0.4367	0.7358	1.0673	0.0533	0.3129	0.1288
Ti	0.3240	0.6049	0.1749	0.4562	0.7202	1.0694	0.0670	0.3143	0.1559
V	0.2937	0.6042	0.1933	0.4593	0.8437	1.0745	0.0753	0.3319	0.1687
Zn	0.3123	0.5888	0.1564	0.4317	0.7111	1.0363	0.0324	0.3157	0.1363
Ag	0.3172	0.5984	0.1399	0.4312	0.7199	1.0034	0.0258	0.3141	0.2932
Cd	0.3120	0.5796	0.1487	0.4176	0.7144	1.0198	0.0278	0.3084	0.1280
In	0.3134	0.5973	0.1458	0.4443	0.7170	1.0666	0.0418	0.3236	0.1610
Mo	0.3052	0.5923	0.1942	0.4668	0.7718	1.0844	0.0745	0.3350	0.1755
Nb	0.2952	0.6071	0.1862	0.4605	0.7505	1.0749	0.0721	0.3274	0.1717
Pd	0.3151	0.6191	0.1872	0.4609	0.7187	1.0525	0.0397	0.3371	0.2963
Rh	0.2870	0.6096	0.2076	0.4297	0.7850	1.0628	0.0604	0.3590	0.2678
Ru	0.3000	0.6040	0.2097	0.4645	0.7812	1.0710	0.0790	0.3319	0.1758
Sb	0.3122	0.6143	0.1436	0.4604	0.7258	1.0938	0.0608	0.3481	0.1912
Sn	0.3132	0.6077	0.1493	0.4550	0.7182	1.0807	0.0517	0.3338	0.1770
Tc	0.3051	0.6025	0.2086	0.4585	0.7777	1.0690	0.0799	0.3285	0.2898
Y	0.3219	0.5847	0.1632	0.4299	0.7245	1.0646	0.0557	0.3182	0.1164
Zr	0.3213	0.5966	0.1669	0.4527	0.7200	1.0620	0.0568	0.3151	0.1510
Au	0.3172	0.5927	0.1448	0.4677	0.7261	0.9827	0.0291	0.2904	0.2898
Bi	0.3108	0.6062	0.1406	0.4521	0.7185	1.0309	0.0528	0.3289	0.1696
Hf	0.3241	0.5981	0.1713	0.4543	0.7236	1.0751	0.0586	0.3142	0.1550
Hg	0.3130	0.5763	0.1421	0.3959	0.7161	0.9951	0.0177	0.2917	0.1258
Ir	0.3054	0.6129	0.2147	0.4199	0.7939	1.0680	0.0712	0.3603	0.1863
Os	0.3033	0.6068	0.2155	0.4695	0.7674	1.0779	0.0823	0.3330	0.1401
Pb	0.3118	0.6044	0.1424	0.4518	0.7199	1.0740	0.0502	0.3250	0.1623
Pt	0.3124	0.6242	0.1985	0.4680	0.7263	1.0514	0.0477	0.3406	0.2725
Re	0.3033	0.6034	0.2108	0.4601	0.7864	1.0807	0.0780	0.3317	0.2191
Ta	0.2938	0.6078	0.1872	0.4601	0.7707	1.0754	0.0732	0.3243	0.1783
Tl	0.3091	0.5948	0.1424	0.4406	0.7123	1.0568	0.0342	0.3173	0.1569
W	0.3066	0.6062	0.1912	0.3984	0.8010	1.0777	0.0787	0.3333	0.1815

Table 12: Entropy corrections ($-T \cdot S$) in eV for relaxed adsorbates supported on graphene with dual-vacancy at 298.15 K.

Metal	*CO ₂	*COOH	*CO	*CHO	*CH ₂ O	*OCH ₃	*O	*OH	*H
Al	-0.2501	-0.2622	-0.1799	-0.2106	-0.3101	-0.2050	-0.0980	-0.1303	-0.0165
Co	-0.1962	-0.2352	-0.1529	-0.1520	-0.1515	-0.0821	-0.0427	-0.1165	-0.0376
Cr	-0.2178	-0.2281	-0.1603	-0.2297	-0.0849	-0.0961	-0.0623	-0.1200	-0.0250
Cu	-0.1907	-0.2528	-0.1276	-0.1239	-0.1974	-0.2279	-0.0711	-0.1357	-0.0044
Fe	-0.2328	-0.2473	-0.0848	-0.1300	-0.1611	-0.1248	-0.0629	-0.0996	-0.0292
Ga	-0.1842	-0.2577	-0.2003	-0.2061	-0.1912	-0.2332	-0.0956	-0.1395	-0.0145
Ge	-0.2491	-0.1850	-0.1442	-0.1942	-0.1974	-0.1522	-0.0886	-0.1119	-0.0101
Mn	-0.2384	-0.2493	-0.1559	-0.1654	-0.1993	-0.1304	-0.0599	-0.1090	-0.0275
Ni	-0.2497	-0.2279	-0.1683	-0.1836	-0.2402	-0.2254	-0.1159	-0.1027	-0.0021
Sc	-0.2252	-0.1996	-0.1449	-0.2023	-0.2586	-0.2259	-0.1128	-0.1670	-0.0322
Ti	-0.2137	-0.2297	-0.1918	-0.1703	-0.2184	-0.2455	-0.0745	-0.1598	-0.0186
V	-0.2319	-0.2441	-0.1693	-0.1713	-0.0933	-0.0952	-0.0673	-0.1171	-0.0164
Zn	-0.1971	-0.2071	-0.1798	-0.2147	-0.1577	-0.2074	-0.1203	-0.1637	-0.0293
Ag	-0.2465	-0.2579	-0.1696	-0.1739	-0.1930	-0.2345	-0.0117	-0.1000	-0.0038
Cd	-0.1963	-0.2145	-0.2124	-0.2350	-0.2120	-0.2341	-0.1338	-0.1754	-0.0354
In	-0.2567	-0.2013	-0.1464	-0.1558	-0.2003	-0.1995	-0.1043	-0.1065	-0.0228
Mo	-0.2106	-0.2086	-0.1656	-0.1746	-0.1628	-0.2038	-0.0668	-0.1129	-0.0144
Nb	-0.2307	-0.2394	-0.1752	-0.1660	-0.1679	-0.1668	-0.0688	-0.1288	-0.0138
Pd	-0.3134	-0.2362	-0.1751	-0.1707	-0.1779	-0.0819	-0.0677	-0.1222	-0.0039
Rh	-0.2128	-0.2468	-0.1542	-0.1986	-0.1595	-0.0720	-0.0949	-0.0933	-0.0021
Ru	-0.2275	-0.2613	-0.1426	-0.1760	-0.1693	-0.0786	-0.0577	-0.1332	-0.0175
Sb	-0.1891	-0.1940	-0.2266	-0.1526	-0.2398	-0.2284	-0.0788	-0.1157	-0.0132
Sn	-0.2529	-0.1968	-0.2028	-0.2165	-0.1898	-0.1845	-0.0886	-0.1568	-0.0170
Tc	-0.2158	-0.2603	-0.1459	-0.1731	-0.1578	-0.0973	-0.0574	-0.1222	-0.0647
Y	-0.2962	-0.2657	-0.1496	-0.2075	-0.2598	-0.2231	-0.1096	-0.1662	-0.0384
Zr	-0.1548	-0.2417	-0.1360	-0.1770	-0.2745	-0.2015	-0.0919	-0.1551	-0.0185
Au	-0.2413	-0.2076	-0.2877	-0.1138	-0.2448	-0.2634	-0.0095	-0.1447	-0.0041
Bi	-0.1970	-0.2006	-0.2337	-0.1648	-0.1315	-0.2394	-0.0927	-0.1399	-0.0183
Hf	-0.2728	-0.2398	-0.1920	-0.1784	-0.2711	-0.3070	-0.0834	-0.1620	-0.0186
Hg	-0.1953	-0.2848	-0.1710	-0.1987	-0.2065	-0.1285	-0.1491	-0.1469	-0.0370
Ir	-0.2144	-0.1796	-0.1476	-0.1609	-0.1474	-0.0751	-0.0699	-0.0953	-0.0258
Os	-0.2163	-0.2409	-0.1420	-0.1599	-0.1776	-0.0816	-0.0565	-0.1218	-0.0724
Pb	-0.1964	-0.2001	-0.2339	-0.1644	-0.1894	-0.1890	-0.0888	-0.1086	-0.0227
Pt	-0.1825	-0.2340	-0.1657	-0.1759	-0.2307	-0.1921	-0.0612	-0.1216	-0.0022
Re	-0.2117	-0.2566	-0.1472	-0.1661	-0.1530	-0.1479	-0.0619	-0.1223	-0.0261
Ta	-0.2269	-0.2462	-0.1744	-0.1715	-0.1696	-0.1787	-0.0694	-0.1428	-0.0135
Tl	-0.1981	-0.2044	-0.2304	-0.2198	-0.2048	-0.2595	-0.1146	-0.1764	-0.0256
W	-0.2006	-0.2433	-0.1670	-0.1453	-0.1295	-0.1025	-0.0613	-0.1185	-0.0157

$$G_{\text{ads}}X = a_X \cdot G_{\text{ads}}\text{CO} + c_X \quad (\text{where } X = \text{COOH, CHO, CH}_2\text{O}) \quad (1)$$

$$G_{\text{ads}}Y = a_Y \cdot G_{\text{ads}}\text{OH} + c_Y \quad (\text{where } Y = \text{O, OCH}_3) \quad (2)$$

Here, CO and OH serve as descriptors for C-centered (X) and O-centered (Y) groups, respectively, and a_X, c_X, a_Y, c_Y are species-specific scaling parameters. The scaling relations simplify the adsorption energy landscape to a two-dimensional space, thereby enabling visualization.

However, it's crucial to note that in the CO₂RR process, most species are not solely C- or O-centered. Thus, it becomes advantageous to incorporate both types of species in the scaling relation. Building upon the hybrid scaling relation introduced in the main text, the free energy change (ΔG) for any given reaction step can be readily calculated using ?? from the main text. Consider the generic reaction step:



The free energy change ΔG is defined as:

$$\Delta G = G({}^*\text{B}) - G({}^*\text{A}) - G(\text{H}^+) - G(\text{e}^-) \quad (4)$$

Focusing on any reaction step delineated by ?? to ?? in the main text, ?? shows that limiting potential U_L at a specific external potential U is fully determined by the adsorption energies of two descriptors. For instance, for the reaction described by ??:

$$\Delta G = G({}^*\text{COOH}) - G({}^*) - G(\text{CO}_2) - G(\text{H}^+) - G(\text{e}^-) \quad (5)$$

$$= G(\text{COOH}) + G({}^*) + G_{\text{ads}}\text{COOH} - G({}^*) - G(\text{CO}_2) - G(\text{H}^+) - G(\text{e}^-) \quad (6)$$

$$= G_{\text{ads}}\text{COOH} + G(\text{COOH}) - G(\text{CO}_2) - G(\text{H}^+) - G(\text{e}^-) \quad (7)$$

From adsorption energy linear relations, we have:

$$G_{\text{ads}}\text{COOH} = a_{\text{COOH}} \cdot G_{\text{ads}}\text{CO} + b_{\text{COOH}} \cdot G_{\text{ads}}\text{OH} + c_{\text{COOH}} \quad (8)$$

which then reduces Supplementary Equation (7) to:

$$\begin{aligned} \Delta G = & (a_{\text{COOH}} \cdot G_{\text{ads}}\text{CO} + b_{\text{COOH}} \cdot G_{\text{ads}}\text{OH}) + \\ & [c_{\text{COOH}} + G(\text{COOH}) - G(\text{CO}_2) - G(\text{H}^+) - G(\text{e}^-)] \end{aligned} \quad (9)$$

In this case, the first term depends solely on the descriptors, while the second term remains constant at a given potential U .

Table 13: Adsorption free energy scaling relation parameters determined by the hybrid descriptor method.

Adsorbate	a_Z	b_Z	c_Z
COOH	0.4032	0.5132	0.0899
CHO	0.5977	0.3664	-2.6763
CH ₂ O	0.5011	0.5011	-0.9806
OCH ₃	0.0532	1.0114	0.8489
O	0.3758	1.2580	0.0910
H	0.3164	0.3568	-0.6764

Note: a_Z , b_Z and c_Z correspond to coefficients for $G_{\text{ads}}\text{CO}$, $G_{\text{ads}}\text{OH}$ and constant terms, where Z stands for the adsorbed species of interest.

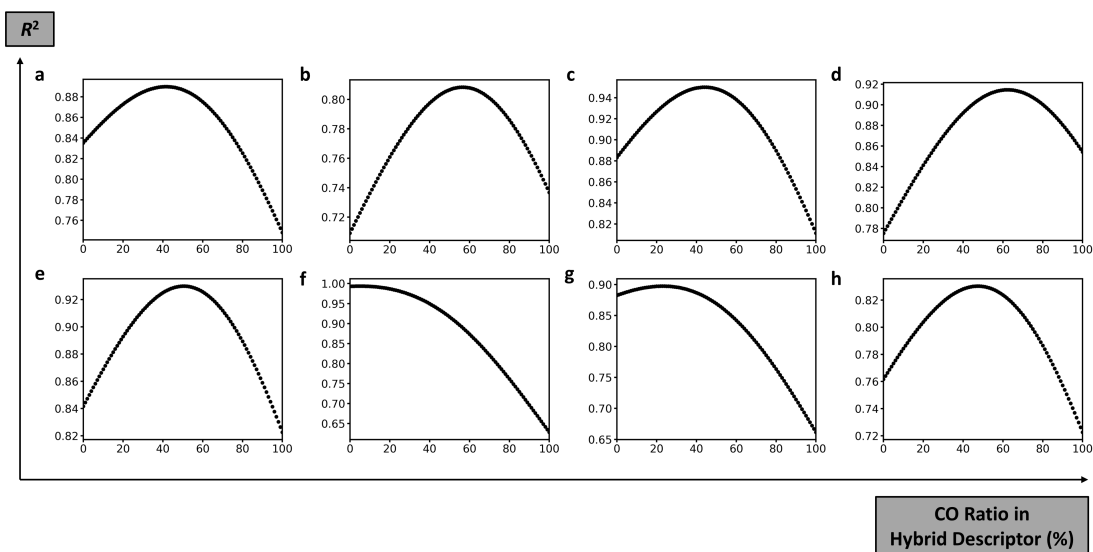


Figure 10: R^2 improvement from hybrid-descriptor method. Improvement in the coefficient of determination (R^2) with x-axis as CO ratio in CO/OH hybrid descriptors. (a) averaged R^2 and those of (b) CO₂, (c) COOH, (d) CHO, (e) CH₂O, (f) OCH₃, (g) O and (h) H are shown.

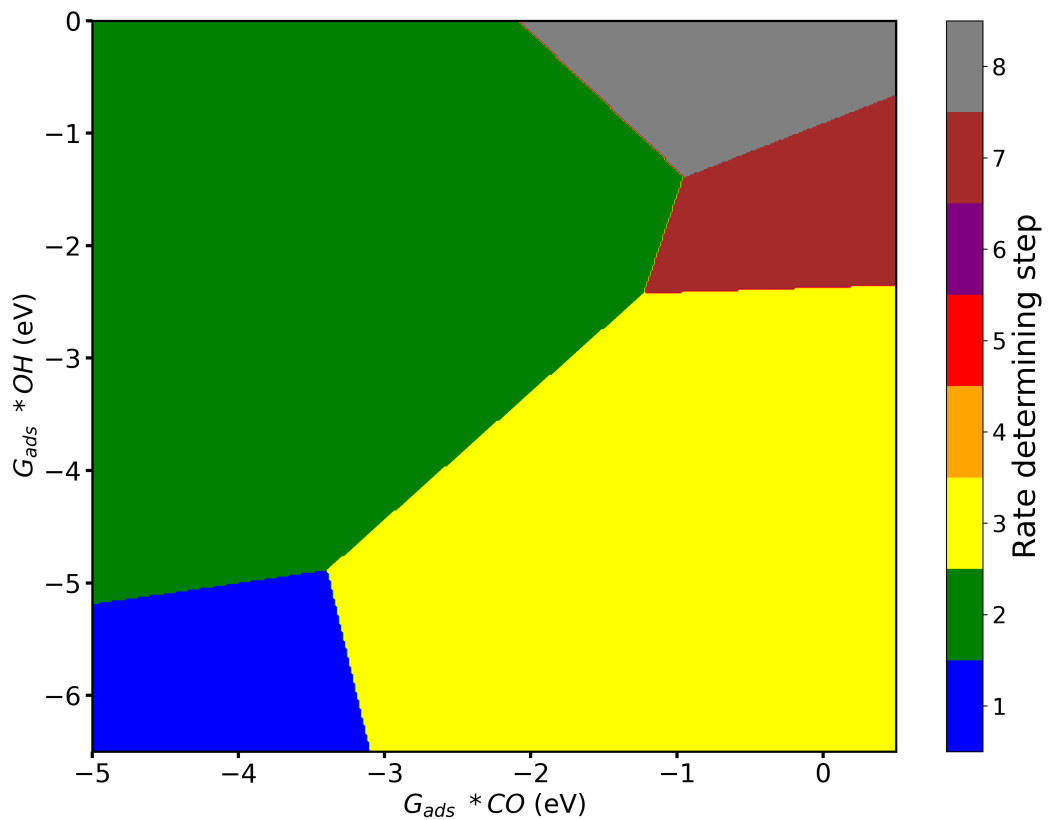


Figure 11: CO₂RR rate determining step volcano plot. This graph illustrates the rate-determining step associated with each region within the CO₂RR process.

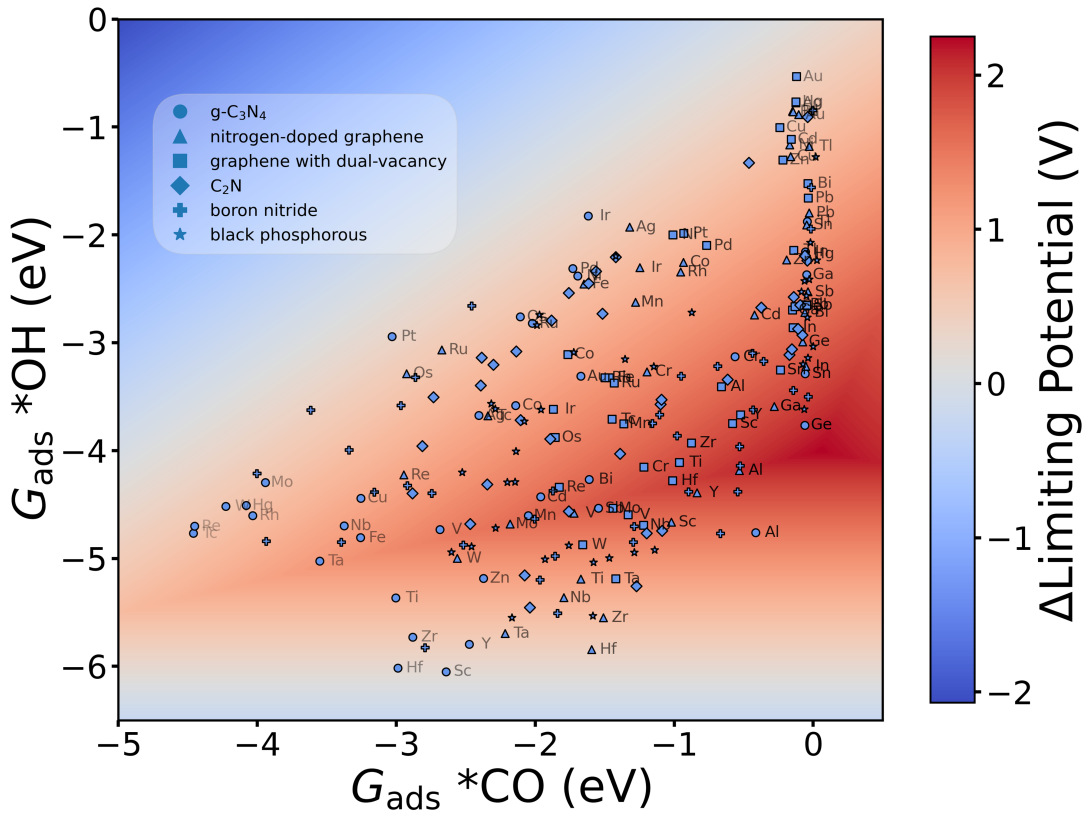


Figure 12: CO₂RR selectivity volcano plot. Selectivity volcano plot computed from linear scaling relations. In the plot, the circle, triangle, square, diamond, plus, and star symbols correspond to metals supported on g-C₃N₄, nitrogen-doped graphene, graphene with dual-vacancy, black phosphorous, BN, and C₂N, respectively.

Table 14: Performance comparison of hybrid descriptor and single descriptor for linear scaling relations.

Adsorbate	Hybrid Descriptor R ² (Optimal CO Ratio)	Single Descriptor R ² Reference Species	R ²
CO ₂	0.8083 (57%)	0.7368 (CO)	0.0715
COOH	0.9500 (44%)	0.8113 (CO)	0.1387
CHO	0.9146 (62%)	0.8541 (CO)	0.0605
CH ₂ O	0.9299 (50%)	0.8226 (CO)	0.1073
OCH ₃	0.9936 (5%)	0.9929 (OH)	0.0007
O	0.8974 (23%)	0.8825 (OH)	0.0149
H	0.8303 (47%)	0.7617 (OH)	0.0686

1.6 Volcano plots

In addition to the selectivity volcano plot featured in the main text, we provide a comprehensive plot capturing all rate-determining steps for CO₂RR in Figure 11. A separate plot focusing on selectivity over HER is also presented in Figure 12.

1.7 Activity periodic tables

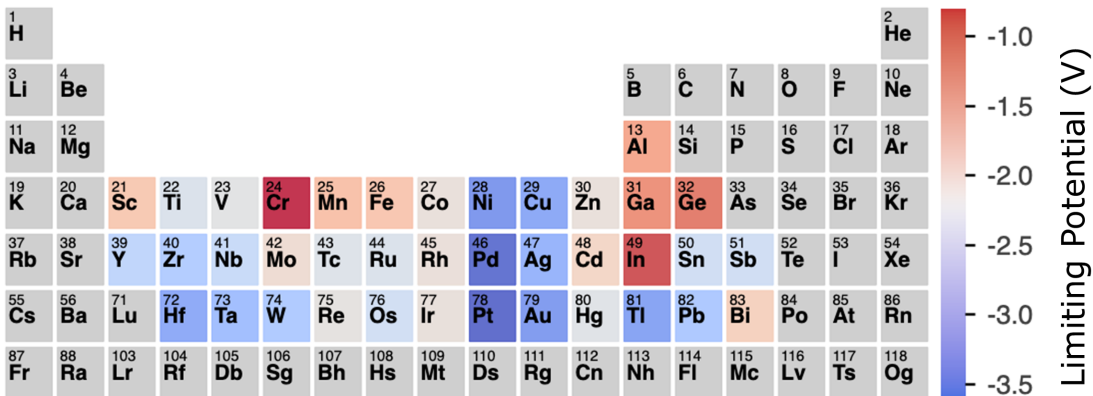


Figure 13: Limiting potential periodic table for nitrogen-doped graphene.

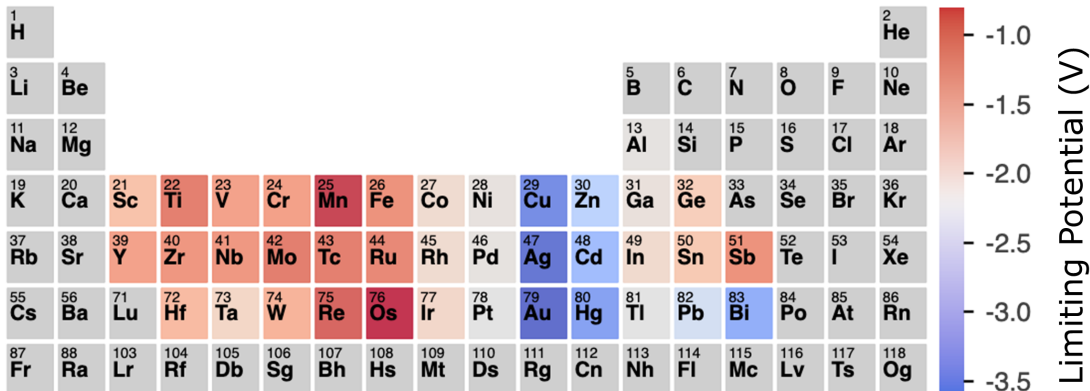


Figure 14: Limiting potential periodic table for graphene with dual-vacancy.

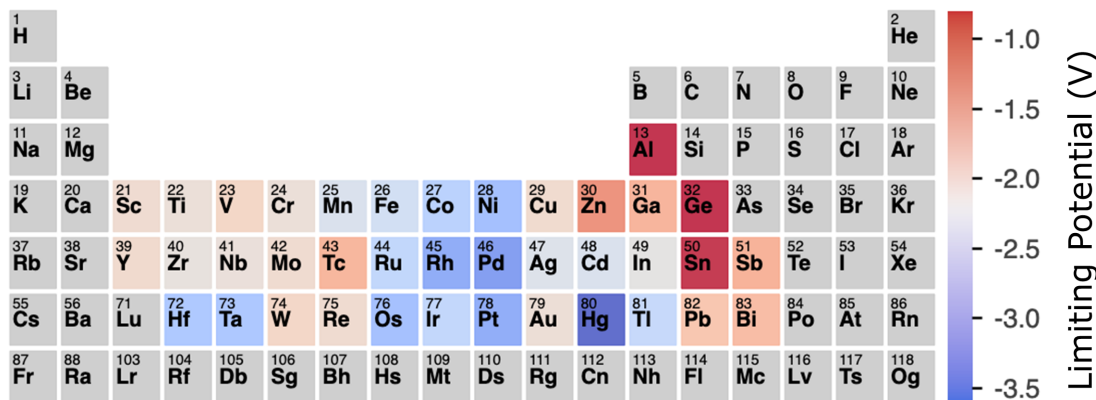


Figure 15: Limiting potential periodic table for black phosphorus.

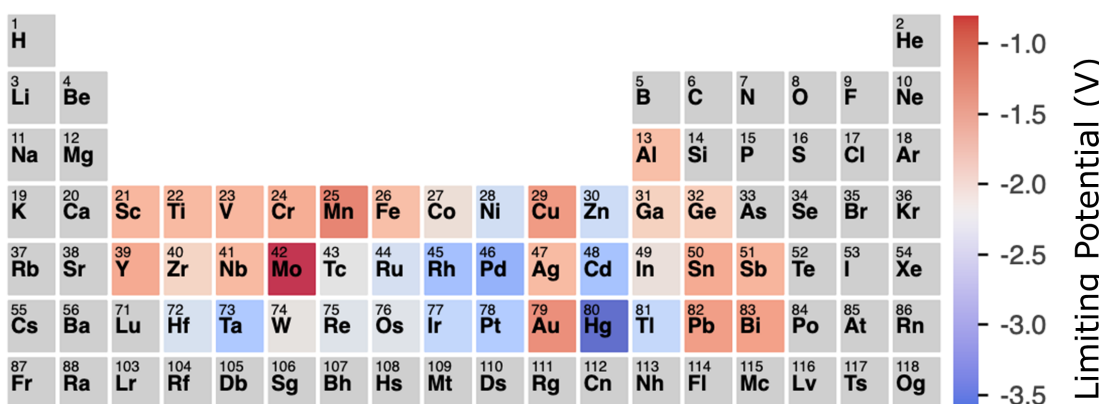


Figure 16: Limiting potential periodic table for boron nitride.

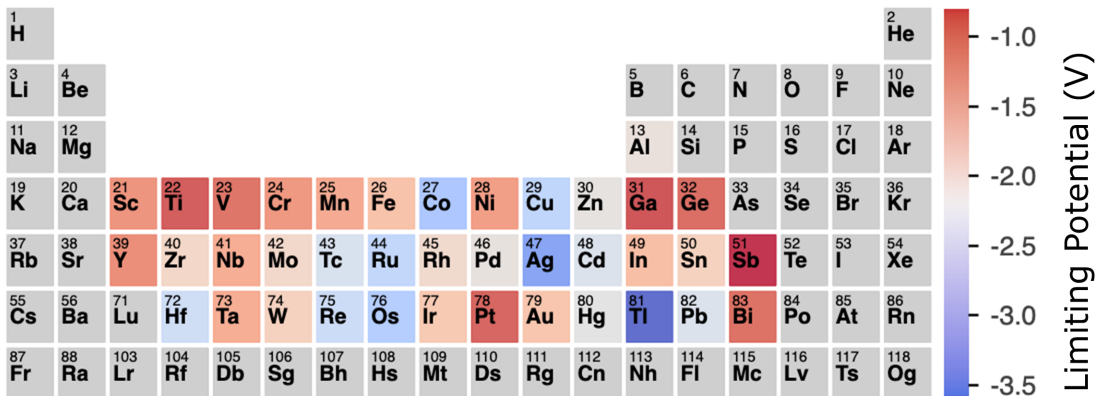


Figure 17: Limiting potential periodic table for monolayer C_2N .

2 Additional details on machine learning method

2.1 d-band center and adsorption energy relations

2.2 Feature correlation analysis

Figure 19 displays the pairwise relationships between CO adsorption energy and its four most correlated descriptors: d-band center (spin-up) $\delta\epsilon_d \uparrow$, lattice parameter γ , vacuum level E_{vac} , and electronegativity on the Allen scale χ_{Allen} , identified by Kendall rank correlation analysis. section 2.2 lists notations for elementary descriptors and electronic descriptors.

Table 15: Notations for elementary descriptors and electronic descriptors.

Elementary Descriptors		Electronic Descriptors	
R	atomic radius	α, β, γ	lattice parameters
E_{ea}	electron affinity	Φ_{DFT}	DFT calculated work function
Φ	work function	E_{vac}	vacuum level
$\chi_{\text{Allen}}, \chi_{\text{P}}, \chi_{\text{RevP}}$	electronegativity in Allen, Pauling and revised Pauling scales	$E_g, E_g \uparrow, E_g \uparrow$	average, spin-up and spin-down band gaps
A_r	relative atomic mass	e_d	number of d-electrons
E_i	ionization energy	$\delta\epsilon_d \uparrow$	d-band centre (spin-up)
G	group number	W_d	d-band width
P	period number	e_{Bader}	Bader charge
V	number of valence electrons		

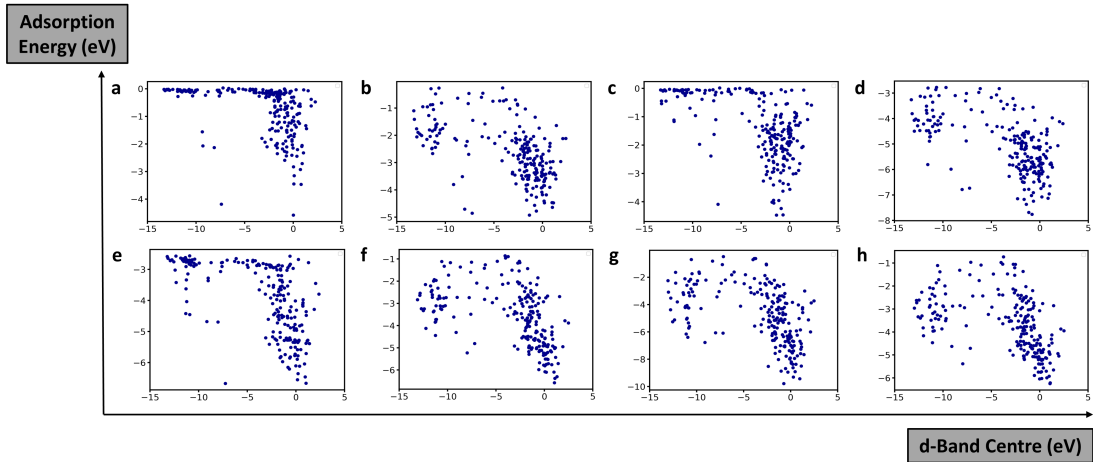


Figure 18: Scatter plot of d-Band Center and Adsorption Energy Relationships. This figure delineates the relationship between d-band center and adsorption energies for various species: (a) CO₂, (b) COOH, (c) CO, (d) CHO, (e) CH₂O, (f) OCH₃, (g) O, and (h) OH. Data from all six substrates investigated in this study are included.

2.3 Input pipeline construction

The format of the 2D array for the eDOS is naturally well-suited for use as neural network inputs. In this study, the array adopts a shape of [numSamplings, numOrbitals, numChannels], as illustrated in Figure 20. Here, “numSamplings” represents the number of data points sampled across the energy spectrum, “numOrbitals” denotes the number of DOS orbitals, and “numChannels” indicates the number of atomic channels.

For practical purposes, certain spatial hierarchies are expected to remain invariant, such as the energy range over which the eDOS is sampled. In this work, we maintain a consistent energy range of -14 eV to 6 eV, sampled at a density of 50 points · eV⁻¹. In addition to maintaining a fixed energy range, the following steps are taken to standardize the input eDOS data: 1. For atoms lacking d-electrons, the eDOS is zero-padded. 2. f-orbital eDOS data are excluded. 3. The eDOS of adsorbates is zero-padded along the Channels axis to align with the adsorbate that contains the maximum number of atoms, which, in this study, is the *OCH₃ species. This padded eDOS is then appended to the metal eDOS.

As a result of these preprocessing steps, the input eDOS arrays consistently have a shape of [4000, 9, 6]. This corresponds to 4000 sampling points across the energy range, 9 eDOS orbitals, and 6 atomic channels.

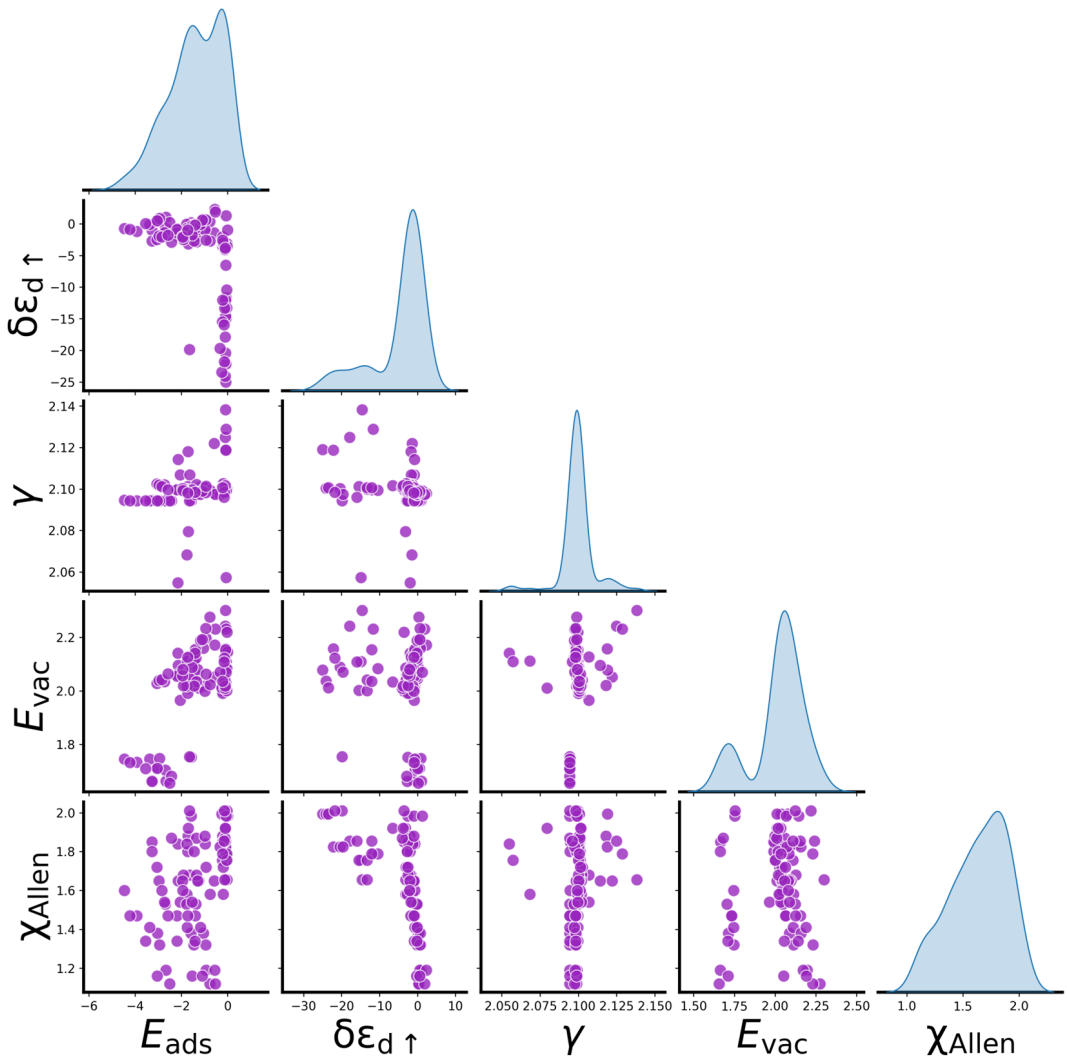


Figure 19: Pairwise Plot of Adsorption Energy and Key Descriptors. This chart displays the pairwise relationships between CO adsorption energy and its four most correlated descriptors: d-band center (spin-up) $\delta\epsilon_d \uparrow$, lattice parameter γ , vacuum level E_{vac} , and electronegativity on the Allen scale χ_{Allen} , identified by Kendall rank correlation analysis. Data from all six substrates investigated in this study are included.

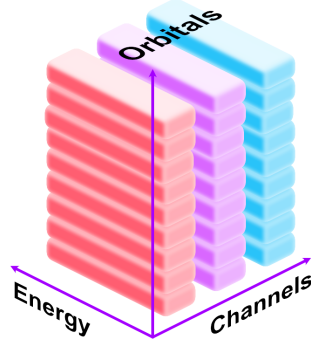


Figure 20: Schematic representation of the input eDOS data structure.

2.4 Hyperparameter tuning for CNN

Table 16: The hyperparameter search space.

Hyperparameter	Search Space	Description
learningRate	$[10^{-4}, 10^{-2}]$, log scale	Learning rate of Adam [3] optimizer
dropoutRate	$[0, 1]$	Dropout rate
root_fc0	128, 256, 512	Output dimensionality of 1 st fully connected layer in root
root_fc1	256, 512, 1024, 2048	Output dimensionality of 2 nd fully connected layer in root
root_act	“tanh”, “relu”, “sigmoid”	Activation function of fully connected layers in root
kernelSize	[2, 32]	Width of the convolution window
numFilters	[8, 64]	Number of filters in the convolution
numConvLayers	[1, 16]	Number of convolution layers
numConvBlocks	[1, 16]	Number of convolution blocks
br_fc0	16, 32, 64, 128, 256, 512	Output dimensionality of 1 st fully connected layer in branch
br_fc1	8, 16, 32, 64, 128, 256	Output dimensionality of 2 nd fully connected layer in branch
br_act	“tanh”, “relu”, “sigmoid”	Activation function of fully connected layers in branch

2.5 Occlusion experiment

2.6 Shifting experiment

Table 17: Optimal hyperparameters identified with Hyperband algorithm.

Hyperparameter	Optimal Value	Description
learningRate	10^{-3}	Learning rate of Adam [3] optimizer
dropoutRate	0.3	Dropout rate
root_fc0	256	Output dimensionality of 1 st fully connected layer in root
root_fc1	512	Output dimensionality of 2 nd fully connected layer in root
root_act	“relu”	Activation function of fully connected layers in root
kernelSize	10	Width of convolution window
numFilters	17	Number of filters in the convolution
numConvLayers	3	Number of convolution layers
numConvBlocks	1	Number of convolution blocks
br_fc0	256	Output dimensionality of 1 st fully connected layer in branch
br_fc1	128	Output dimensionality of 2 nd fully connected layer in branch
br_act	“tanh”	Activation function of fully connected layers in branch

Table 18: Prediction mean absolute errors of the CNN model.

Adsorbate	Original dataset (eV)	Augmented dataset (eV)
CO ₂	0.0447	0.0336
COOH	0.0436	0.0581
CO	0.0402	0.0402
CHO	0.0614	0.0778
CH ₂ O	0.0553	0.0632
OCH ₃	0.0605	0.0636
O	0.1135	0.1081
OH	0.0547	0.0602
H	0.0703	0.0646

Note: The same CNN model, trained on the augmented dataset, was used for all predictions. The term “original dataset” refers to evaluations conducted on the original dataset without any augmented data; it does not imply the use of a different CNN model trained solely on the original dataset. Similarly, “augmented dataset” refers to evaluations on the dataset with both original data and augment data, not a distinct model.

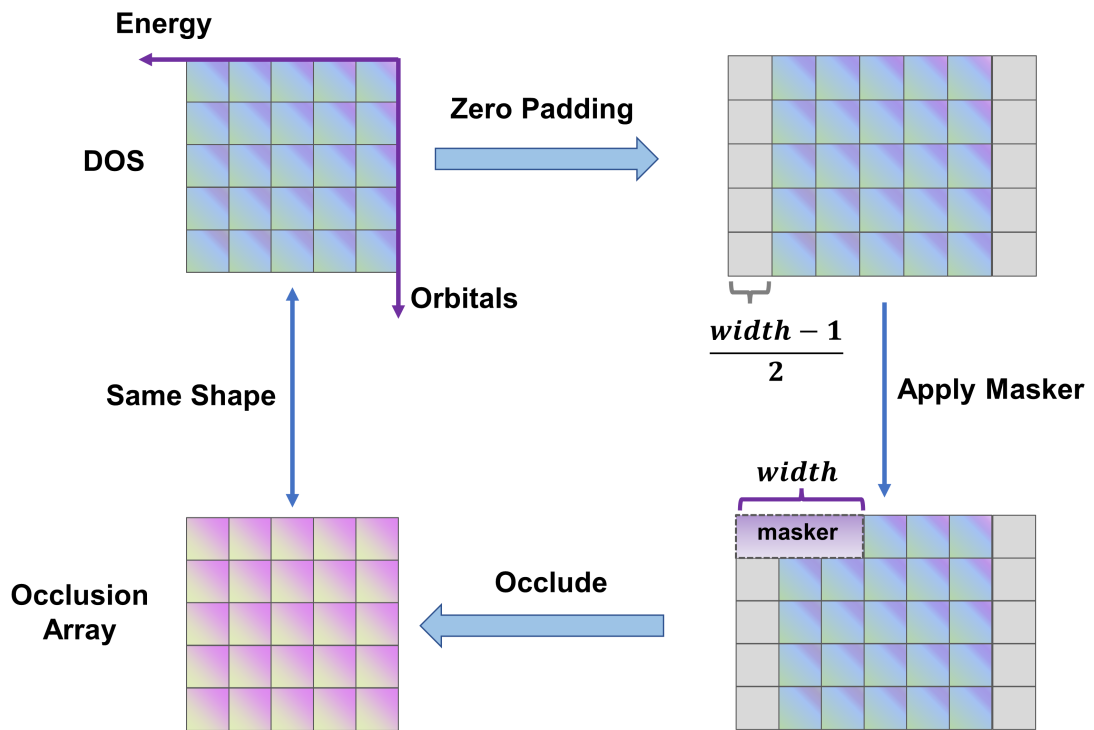


Figure 21: Illustration of the eDOS occlusion experiment. This figure demonstrates the step-by-step process of the occlusion experiment. The input eDOS array first undergoes zero-padded, and then a masker of width “width” is applied, resulting in an occlusion array that preserves the shape of the input array.

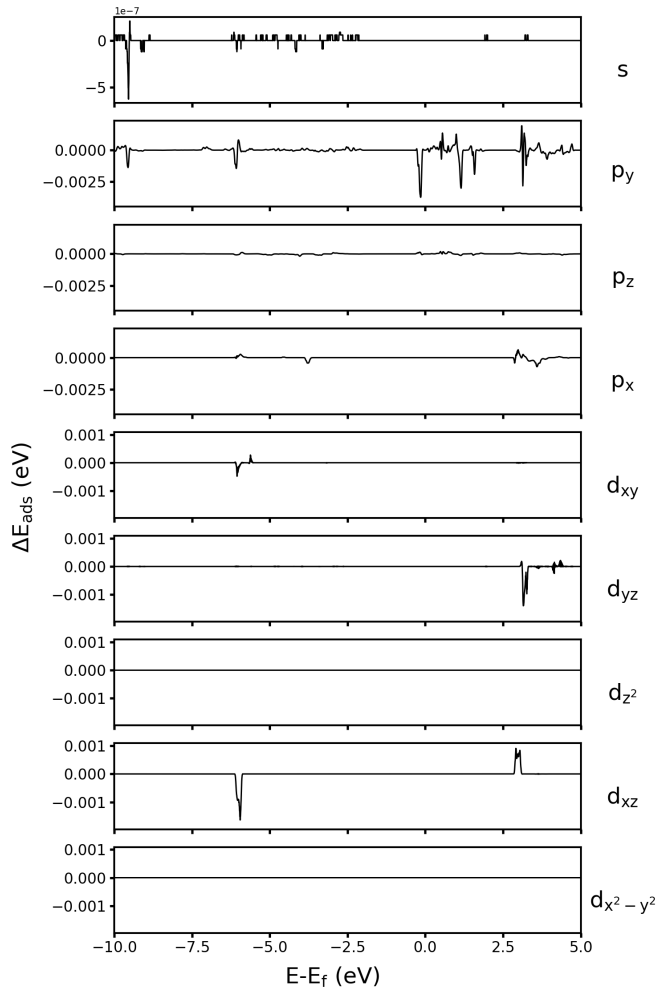


Figure 22: Occlusion Experiment with a masker width of “1”. This figure shows an occlusion experiment on the Ge atom in the initial state of CO adsorption on Ge@g-C₃N₄.

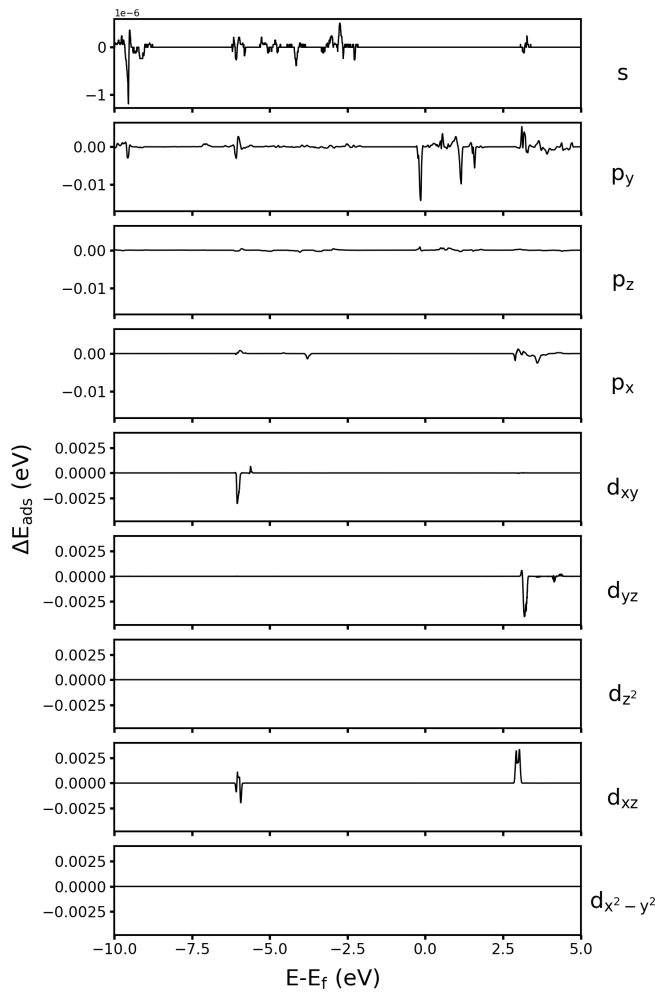


Figure 23: Occlusion Experiment with a masker width of “3”. This figure shows an occlusion experiment on the Ge atom in the initial state of CO adsorption on Ge@g-C₃N₄.

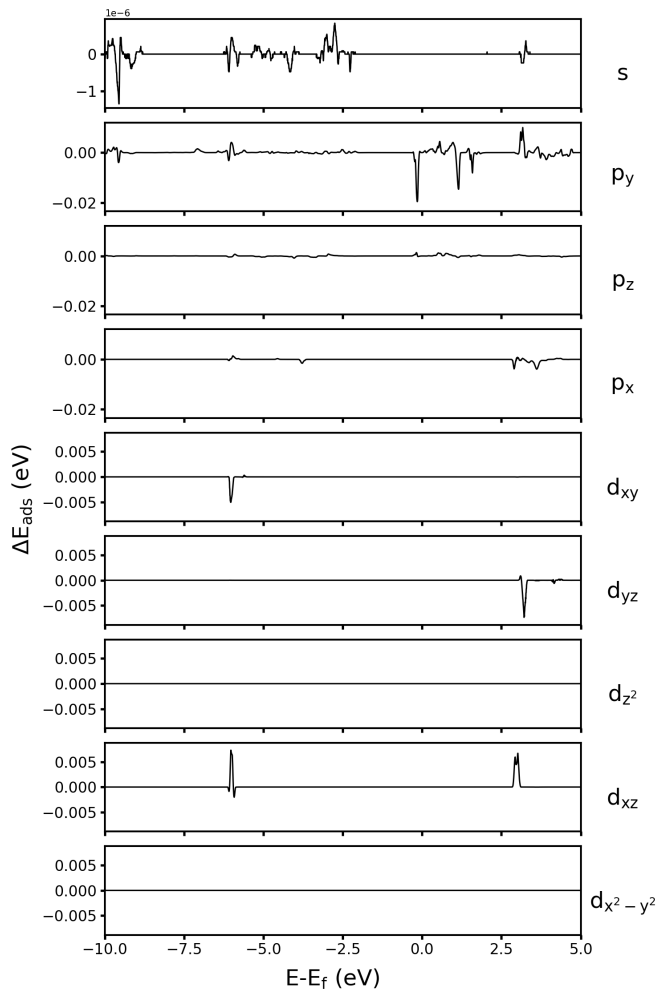


Figure 24: Occlusion Experiment with a masker width of “5”. This figure shows an occlusion experiment on the Ge atom in the initial state of CO adsorption on Ge@g-C₃N₄.

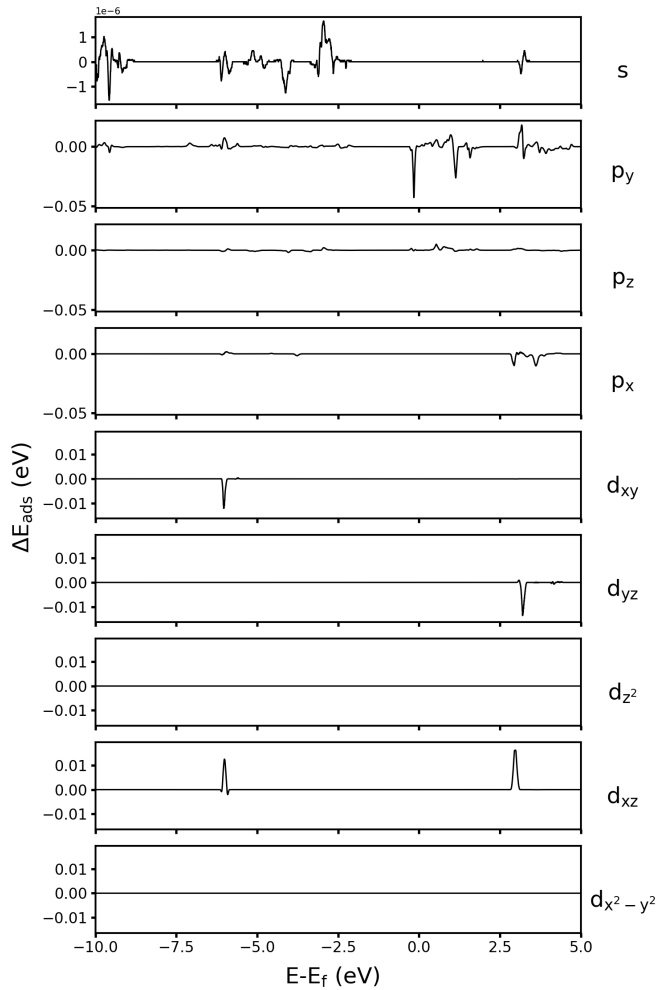


Figure 25: Occlusion Experiment with a masker width of “11”. This figure shows an occlusion experiment on the Ge atom in the initial state of CO adsorption on Ge@g-C₃N₄.

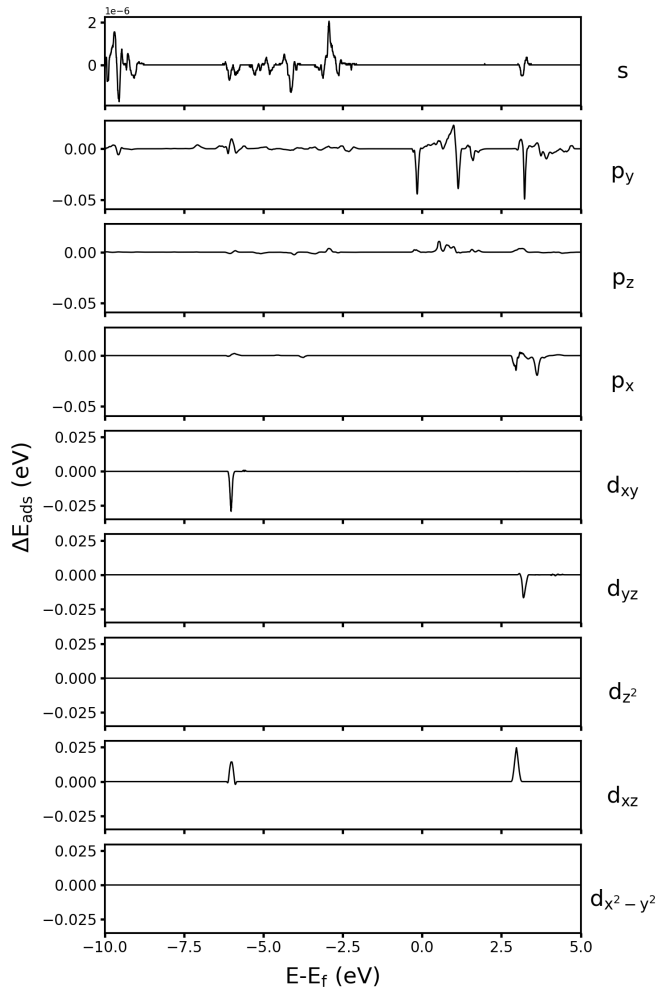


Figure 26: Occlusion Experiment with a masker width of “21”. This figure shows an occlusion experiment on the Ge atom in the initial state of CO adsorption on Ge@g-C₃N₄.

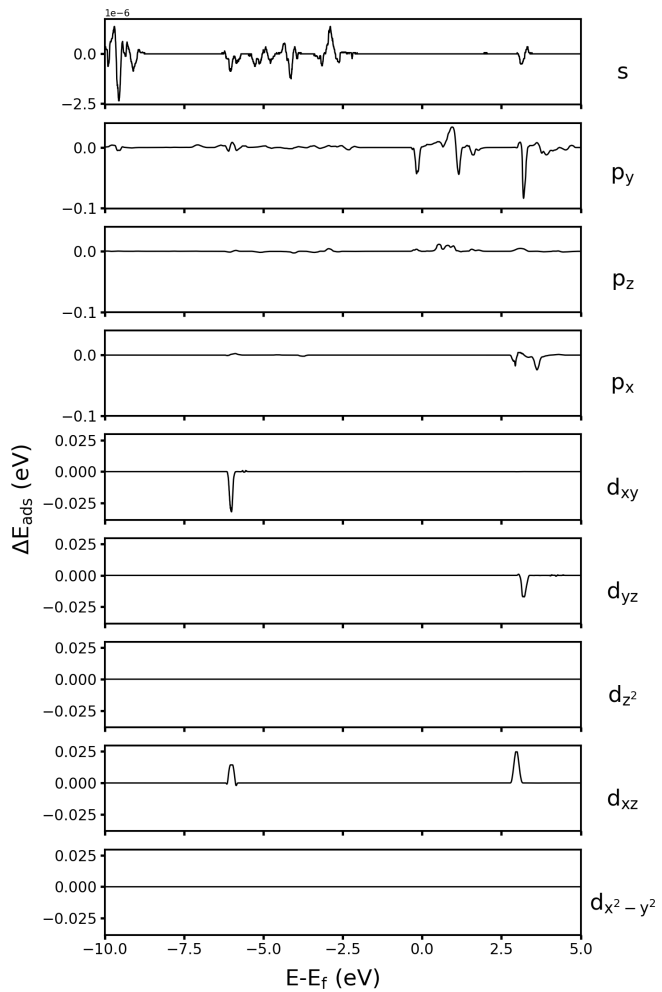


Figure 27: Occlusion Experiment with a masker width of “31”. This figure shows an occlusion experiment on the Ge atom in the initial state of CO adsorption on Ge@g-C₃N₄.

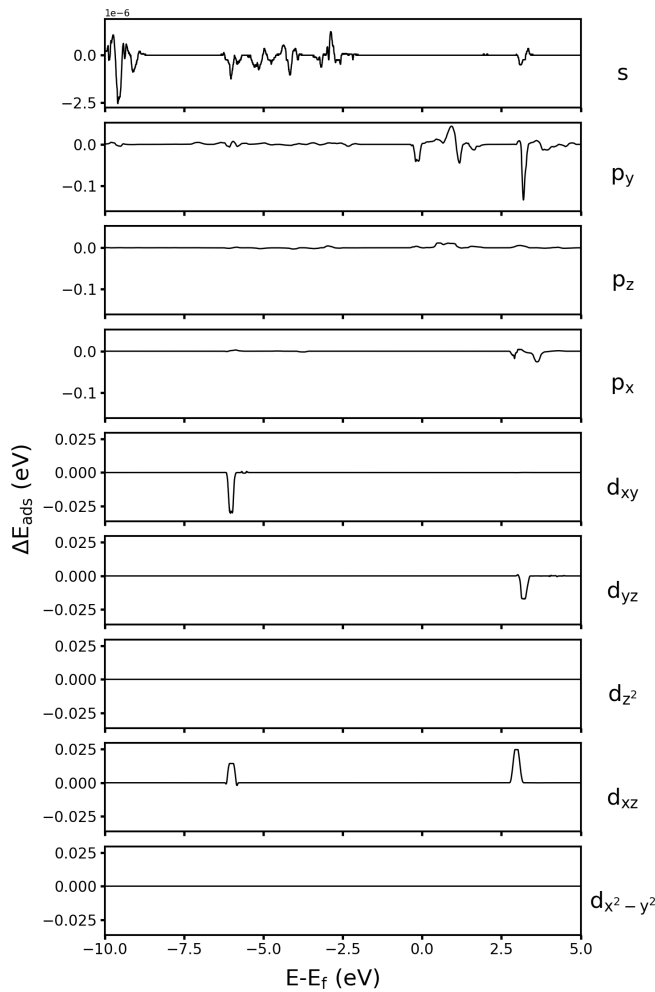


Figure 28: Occlusion Experiment with a masker width of “41”. This figure shows an occlusion experiment on the Ge atom in the initial state of CO adsorption on Ge@g-C₃N₄.

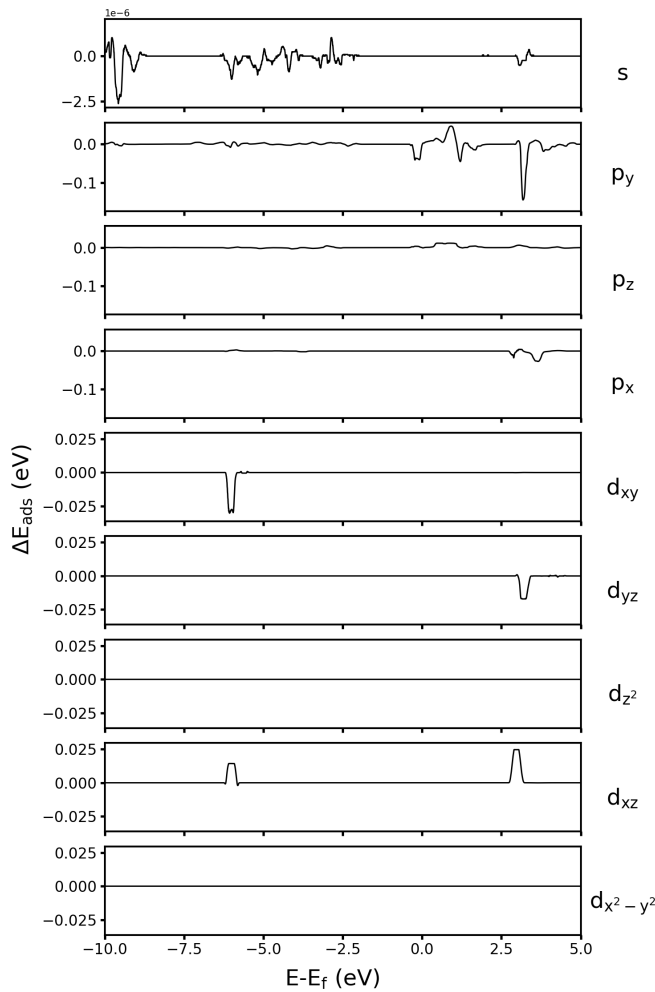


Figure 29: Occlusion Experiment with a masker width of “51”. This figure shows an occlusion experiment on the Ge atom in the initial state of CO adsorption on Ge@g-C₃N₄.

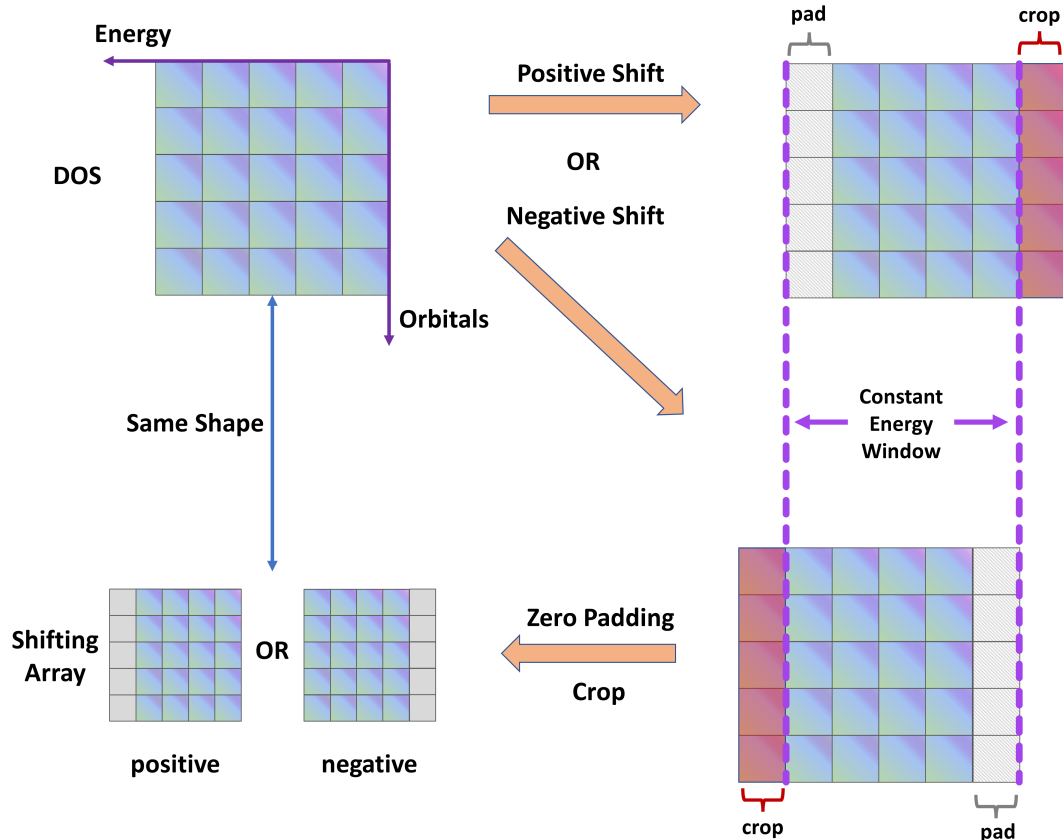


Figure 30: Illustration of the eDOS shifting experiment. This figure illustrates the sequential stages of the shifting experiment. Initially, the input eDOS array is shifted along the Energy axis. Subsequently, it undergoes zero-padding and cropping, ensuring a consistent shape based on the shifting direction, to match the input eDOS array. The resulting shifted array is then processed by the CNN model to assess the disturbance in adsorption energy caused by the shifting operation.

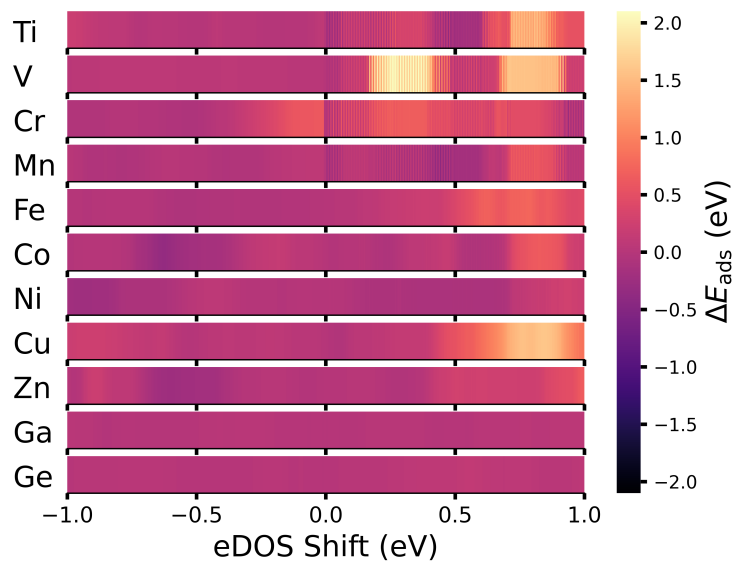


Figure 31: Shifting experiment on p orbital. Effect of orbital shifting on CO adsorption energy, predicted by the CNN model, for single metal atom catalysts supported on g-C₃N₄. The perturbations caused by shifting of entire p orbital are presented. The shifting step size corresponds to the energy resolution of the eDOS, set at 0.005 eV in this study. A positive eDOS shift indicates a shift towards higher energy levels, and vice versa.

3 Other additional information

3.1 Additional information on machine learning environment

The hyperparameter optimization for the proposed CNN model was performed using NVIDIA® V100 Tensor Core GPUs, courtesy of the Australian National Computational Infrastructure’s (NCI) HPC Gadi system. The HyperBand algorithm [4], as implemented in KerasTuner [6], facilitated the tuning process.

Table 19: Core packages in the deep learning environment.

Name	Version	Build	Channel
conda	4.13.0	py39h06a4308_0	anaconda
cuda-nvcc	11.8.89	0	nvidia
cuda-toolkit	11.8.0	0	nvidia
cudatoolkit	11.6.0	habf752d_9	nvidia
ipykernel	6.9.1	py39h06a4308_0	anaconda
ipython	7.34.0	pypi_0	pypi
jupyter_client	7.2.2	py39h06a4308_0	anaconda
jupyterlab	3.4.4	py39h06a4308_0	anaconda
keras	2.9.0	pypi_0	pypi
keras-preprocessing	1.1.2	pypi_0	pypi
keras-tuner	1.3.5		pypi
matplotlib	3.5.1	py39h06a4308_1	anaconda
numpy	1.22.4	pypi_0	pypi
pandas	1.3.4	py39h8c16a72_0	anaconda
python	3.9.12	h12debd9_1	anaconda
scikit-learn	1.1.1	py39h6a678d5_0	anaconda
scipy	1.8.1	py39hddc5342_3	conda-forge
tensorboard	2.9.1	pypi_0	pypi
tensorflow	2.9.3	pypi_0	pypi
tensorflow-gpu	2.9.3	pypi_0	pypi
xlrd	2.0.1	pyhd3eb1b0_0	anaconda
yaml	0.2.5	h7b6447c_0	anaconda

Note: The complete list of packages is provided along with the source code.

3.2 Additional information on data analysis and visualization environment

Data analysis and visualization tasks were executed on an Apple MacBook Air featuring an octa-core M2 chip. For accuracy, the TensorFlow-Metal plugin for Mac-based GPU acceleration was deliberately excluded, as it could potentially yield erroneous CNN model predictions.

The illustrations of CNN architecture displayed in ?? of the main text, as well as Figure 21 and Figure 30, were obtained from the GitHub repository dair-ai/ml-visuals [9]. Blender was used to create and render the visual representation of the catalyst analysis pipeline shown in ?? of the main text.

Table 20: Core packages in data analysis and visualization environment.

Name	Version	Build	Channel
bokeh	3.2.2	pypi_0	pypi
colorcet	3.0.1	pypi_0	pypi
heatmapz	0.0.4	pypi_0	pypi
keras	2.13.1	pypi_0	pypi
keras-tuner	1.3.5	pypi_0	pypi
matplotlib	3.7.2	pypi_0	pypi
numpy	1.24.3	pypi_0	pypi
pandas	2.0.3	pypi_0	pypi
python	3.11.4	hb885b13_0	
pyyaml	6.0.1	pypi_0	pypi
scikit-learn	1.3.0	pypi_0	pypi
scipy	1.11.1	pypi_0	pypi
seaborn	0.12.2	pypi_0	pypi
tensorboard	2.13.0	pypi_0	pypi
tensorflow	2.13.0	pypi_0	pypi
tensorflow-macos	2.13.0	pypi_0	pypi

Note: The complete list of packages is provided along with the source code.

References

- [1] Frank Abild-Pedersen, Jeff Greeley, Felix Studt, Jan Rossmeisl, Ture R Munter, Poul Georg Moses, Egill Skulason, Thomas Bligaard, and Jens Kehlet Nørskov. Scaling properties of adsorption energies for hydrogen-containing molecules on transition-metal surfaces. *Physical review letters*, 99(1):016105, 2007.
- [2] William J Durand, Andrew A Peterson, Felix Studt, Frank Abild-Pedersen, and Jens K Nørskov. Structure effects on the energetics of the electrochemical reduction of co₂ by copper surfaces. *Surface Science*, 605(15-16):1354–1359, 2011.
- [3] Diederik P. Kingma and Jimmy Ba. Adam: A method for stochastic optimization, 2017.
- [4] Lisha Li, Kevin Jamieson, Giulia DeSalvo, Afshin Rostamizadeh, and Ameet Talwalkar. Hyperband: A novel bandit-based approach to hyperparameter optimization. *Journal of Machine Learning Research*, 18(185):1–52, 2018.
- [5] Xiaowa Nie, Wenjia Luo, Michael J Janik, and Aravind Asthagiri. Reaction mechanisms of co₂ electrochemical reduction on cu (1 1 1) determined with density functional theory. *Journal of catalysis*, 312:108–122, 2014.
- [6] Tom O’Malley, Elie Bursztein, James Long, François Chollet, Haifeng Jin, Luca Invernizzi, et al. Kerastuner. <https://github.com/keras-team/keras-tuner>, 2019.
- [7] Andrew A Peterson, Frank Abild-Pedersen, Felix Studt, Jan Rossmeisl, and Jens K Nørskov. How copper catalyzes the electroreduction of carbon dioxide into hydrocarbon fuels. *Energy & Environmental Science*, 3(9):1311–1315, 2010.
- [8] Andrew A Peterson and Jens K Nørskov. Activity descriptors for co₂ electroreduction to methane on transition-metal catalysts. *The Journal of Physical Chemistry Letters*, 3(2):251–258, 2012.
- [9] Elvis Saravia. ML Visuals. <https://github.com/dair-ai/ml-visuals>, December 2021.
- [10] Vei Wang, Nan Xu, Jin-Cheng Liu, Gang Tang, and Wen-Tong Geng. Vaspkit: A user-friendly interface facilitating high-throughput computing and analysis using vasp code. *Computer Physics Communications*, 267:108033, 2021.